Cell Reports

Article

Metabolism of glucose activates TORC1 through multiple mechanisms in *Saccharomyces cerevisiae*

Graphical abstract

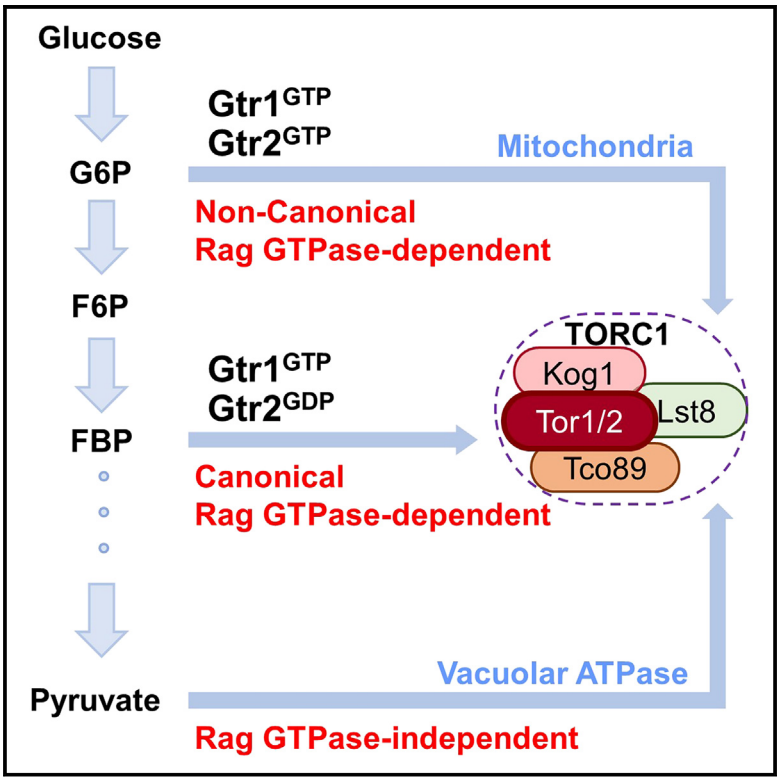

Highlights

- Glucose metabolism activates TORC1 in *S. cerevisiae* via at least three distinct pathways
- Phosphorylation of glucose to G6P activates TORC1 through $Gtr1^{GTP}$-$Gtr2^{GTP}$
- Conversion of glucose to FBP activates TORC1 through $Gtr1^{GTP}$-$Gtr2^{GDP}$
- Complete glycolysis activates TORC1 independent of Rag GTPases (Gtr1/Gtr2)

Authors

Mohammad Alfatah, Liang Cui, Corinna Jie Hui Goh, ..., Jacqueline Lewis, Wei Jie Poh, Prakash Arumugam

Correspondence

alfatahm@bii.a-star.edu.sg (M.A.), parumugam@sifbi.a-star.edu.sg (P.A.)

In brief

Alfatah et al. interrogate the relationship between glucose metabolism and TORC1 activation in *Saccharomyces cerevisiae*. They identify three distinct pathways for glucose-induced TORC1 activation, with each pathway requiring a different extent of glucose metabolism via the glycolytic pathway.

Alfatah et al., 2023, Cell Reports *42*, 113205
October 31, 2023
https://doi.org/10.1016/j.celrep.2023.113205

CellPress

Cell Reports

CellPress
OPEN ACCESS

Article

Metabolism of glucose activates TORC1 through multiple mechanisms in *Saccharomyces cerevisiae*

Mohammad Alfatah,[1,*] Liang Cui,[2] Corinna Jie Hui Goh,[1] Trishia Yi Ning Cheng,[1] Yizhong Zhang,[1] Arshia Naaz,[3] Jin Huei Wong,[1] Jacqueline Lewis,[4] Wei Jie Poh,[1] and Prakash Arumugam[5,6,7,*]

[1]Bioinformatics Institute, A*STAR, 30 Biopolis Street, Singapore 138671, Singapore
[2]Antimicrobial Resistance Interdisciplinary Research Group, Singapore-MIT Alliance for Research and Technology, 1 CREATE Way, Singapore 138602, Singapore
[3]Genome Institute of Singapore, A*STAR, 60 Biopolis Street, Genome #02-01, Singapore 138672, Singapore
[4]Institute of Molecular and Cellular Biology, 61 Biopolis Drive, Singapore 138673, Singapore
[5]Singapore Institute of Food and Biotechnology Innovation, A*STAR, 31 Biopolis Way, Singapore 138669, Singapore
[6]Nanyang Technological University, School of Biological Sciences, Singapore 637551, Singapore
[7]Lead contact
*Correspondence: alfatahm@bii.a-star.edu.sg (M.A.), parumugam@sifbi.a-star.edu.sg (P.A.)
https://doi.org/10.1016/j.celrep.2023.113205

SUMMARY

Target of Rapamycin Complex 1 (TORC1) is a conserved eukaryotic protein complex that links the presence of nutrients with cell growth. In *Saccharomyces cerevisiae*, TORC1 activity is positively regulated by the presence of amino acids and glucose in the medium. However, the mechanisms underlying nutrient-induced TORC1 activation remain poorly understood. By utilizing an *in vivo* TORC1 activation assay, we demonstrate that differential metabolism of glucose activates TORC1 through three distinct pathways in yeast. The first "canonical Rag guanosine triphosphatase (GTPase)-dependent pathway" requires conversion of glucose to fructose 1,6-bisphosphate, which activates TORC1 via the Rag GTPase heterodimer $Gtr1^{GTP}$-$Gtr2^{GDP}$. The second "non-canonical Rag GTPase-dependent pathway" requires conversion of glucose to glucose 6-phosphate, which activates TORC1 via a process that involves $Gtr1^{GTP}$-$Gtr2^{GTP}$ and mitochondrial function. The third "Rag GTPase-independent pathway" requires complete glycolysis and vacuolar ATPase reassembly for TORC1 activation. We have established a roadmap to deconstruct the link between glucose metabolism and TORC1 activation.

INTRODUCTION

Target of Rapamycin Complex 1 (TORC1) is a master regulator of eukaryotic cell growth, proliferation, and metabolism. The TORC1 signaling pathway controls cellular growth through activation of anabolic processes such as protein, lipid, and nucleotide synthesis and repression of catabolic processes such as autophagy and proteasomal activity. Dysregulation of TORC1 signaling has been implicated in a diverse set of common human diseases, including cancer, neurological disorders, obesity, and diabetes.

TORC1 is a serine/threonine protein kinase belonging to the phosphatidylinositol 3-kinase (PI3K)-related family of lipid kinases. The *Saccharomyces cerevisiae* TORC1 is composed of four subunits: Tor1 or Tor2 (the catalytic subunit), Kog1 (ortholog of mammalian raptor), Lst8 (synthetic lethal with sec thirteen), and Tco89.[1] TORC1 in yeast forms a lozenge-shaped dimer that contains two copies of each of the 4 subunits. Human mTORC1's composition is similar to its yeast counterpart but lacks Tco89.

TORC1 is regulated by the conserved Rag family of small guanosine triphosphatases (GTPases); namely, the Gtr1 (RagA/B) and Gtr2 (RagC/D) proteins in yeast.[2] Gtr1 and Gtr2 heterodimerize and localize to vacuolar membranes via an interaction with the EGO (Ego1-Ego2-Ego3) complex.[3] Amino acid sufficiency promotes the active conformation of the Gtr1/Gtr2 heterodimer, in which Gtr1 and Gtr2 are loaded with guanosine triphosphate (GTP) and guanosine diphosphate (GDP), respectively.[4] The active $Gtr1^{GTP}$-$Gtr2^{GDP}$ heterodimer binds to Kog1 and activates TORC1. Mammalian RagA/B and RagC/D GTPases bind to the lysosomal Ragulator complex composed of five subunit proteins (LAMTOR1–LAMTOR5) and sense the availability of amino acids.[5] In the presence of amino acids (particularly leucine and arginine), RagA/B and RagC/D GTPases activate mTORC1 by recruiting it to the lysosomes for activation by the lysosomal Rheb GTPase. Notably, mTORC1, but not the budding yeast TORC1, is regulated by the Rheb GTPase. Budding yeast TORC1 localizes mainly to the vacuoles in a constitutive manner.[6,7] However, mTORC1 requires Rag-GTPases for its lysosomal localization.[8]

The nucleotide-binding status of Gtr1 and Gtr2 is tightly regulated by conserved GAPs (GTPase-activating proteins) and GEFs (guanine exchange factors). EACIT (Seh1-Associated Complex Inhibiting TORC1 signaling) and Lst4-Lst7 complexes act as GAPs for Gtr1 and Gtr2, respectively.[9] Budding yeast SEACIT contains three subunits, namely Iml1, Npr2, and Npr3. The activity of SEACIT is negatively regulated by the

SEACAT (Seh1-Associated Complex Activating TORC1 signaling) complex in yeast.[4] SEACAT is composed of five subunits, namely Sea2, Sea3, Sea4, Seh1, and Sec13. The mammalian counterparts for SEACIT and SEACAT are GATOR1 and GATOR2 complexes, respectively. The budding yeast vacuolar protein Vam6 has been proposed to be the GEF for Gtr1.[4] Vam6 is a component of the conserved HOPS (Homotypic fusion and Protein Sorting) complex involved in homotypic vacuolar fusion and vacuolar protein sorting. The identity of the GEF for Gtr2 remains unknown. Despite differences in subunit composition and regulatory mechanisms, both yeast and mammalian TORC1 complexes share the common cellular function of coordinating extracellular signals with protein translation and catabolism.

It is intriguing how nutrients regulate TORC1 activity in eukaryotic cells. Somewhat unexpectedly, this process is better understood in mammalian cells in comparison with yeast. In the absence of amino acids, sestrins bind and inhibit mammalian GATOR2.[10–13] This frees up GATOR1, which activates GTP hydrolysis on RagA/B and inhibits mTORC1. Binding of amino acids like leucine and arginine to sestrins inhibits its interaction with GATOR2 and activates mTORC1. Apart from one report showing that the leucyl tRNA synthetase (Cdc60) acts as a GEF for Gtr1 in a leucine-dependent manner,[14] there is very little progress in understanding how nutrients activate TORC1 in *S. cerevisiae*.

TORC1 activity in yeast is highly sensitive to the presence of glucose.[15–18] The availability of glucose regulates disassembly/reassembly of vacuolar ATPase (V-ATPase).[19] V-ATPase has been proposed to activate TORC1 in response to glucose and amino acids via Gtr1.[20] Specifically, in response to glucose but not nitrogen starvation, TORC1 has been reported to disassemble, with its Raptor subunit Kog1 relocating to the vacuolar edge to form Kog1 bodies.[18] Formation of Kog1 bodies is driven by Snf1-AMPK(Adenosine Monophosphate-activated Protein Kinase)-mediated phosphorylation of Kog1 at Ser 491/494 and two adjacent prion motifs.[18] When budding yeast cells were subjected to glucose starvation, TORC1 has been reported to form catalytically inactive cylindrical structures called TOROIDs (TORC1 oligomerized in inhibited domain), perched on the vacuolar membrane.[21] While the inactive $Gtr1^{GDP}$-$Gtr2^{GTP}$ promotes TOROID formation, the active $Gtr1^{GTP}$-$Gtr2^{GDP}$ antagonizes their formation.[21] Unlike observed for Kog1 bodies, the Snf1/AMPK did not regulate TOROID formation.[21]

We recently showed that glucose activates TORC1 via Rag GTPase-dependent and Rag GTPase-independent mechanisms.[16] In this study, we combined genetics with targeted metabolite analysis to determine the extent of glucose metabolism and the upstream TORC1 regulators required for glucose-induced TORC1 activation. We show that glucose activates TORC1 through three distinct pathways. In the first pathway, formation of fructose 1,6-bisphosphate activates TORC1 via the canonical pathway dependent on $Gtr1^{GTP}$-$Gtr2^{GDP}$. In the second pathway, formation of glucose 6-phosphate activates TORC1 non-canonical pathway involving $Gtr1^{GTP}$-$Gtr2^{GTP}$ and requiring mitochondrial function. Complete glycolysis of glucose to pyruvate activates TORC1 via the third Rag GTPase-independent pathway, and this requires V-ATPase reassembly and activity. Our work indicates that yeast cells have evolved multiple mechanisms to link glycolysis with growth, providing an explanation for their well-known preference for glucose as a carbon source.

RESULTS

Hexokinase-mediated phosphorylation of glucose is essential for glucose-induced TORC1 activation

We have demonstrated previously that glucose is sufficient to activate TORC1 via Rag GTPase-dependent and Rag GTPase-independent mechanisms in *S. cerevisiae*.[16] In the glucose-induced TORC1 activation assay, log-phase yeast cells are subjected to complete nutrient starvation by incubating them in water for 1 h. Glucose is then added to starved cultures, and TORC1 activity is assessed by monitoring phosphorylation of its substrate, Sch9.[16] Glucose can either directly activate TORC1 or it might have to be metabolized to activate TORC1. We first tested whether glucose is metabolized by yeast cells during the conditions of our glucose-induced TORC1 activation assay. We performed the glucose-induced TORC1 activation assay with wild-type and *gtr1Δ* cells and measured the relative levels of glycolytic intermediates by liquid chromatography (LC)-mass spectrometry (MS) (Figure 1A). In starved cells, lower glycolytic intermediates, such as phosphoenolpyruvate (PEP) and 2-phosphoglycerate (2-PG)/3-phosphoglycerate (3-PG) accumulated (Figure 1A), which is consistent with a previous study.[22] Upon addition of 2% glucose to starved cells, the relative molar levels of glucose 6-phosphate (G6P), fructose 6-phosphate (F6P), fructose 1,6-bisphosphate (FBP), and glyceraldehyde-3-phosphate (G3P)/dihydroxyacetone phosphate (DHAP) increased and the relative molar levels of PEP and 2PG/3PG decreased (Figure 1A). These results demonstrate that glucose undergoes glycolysis in yeast cells under the conditions of the glucose-induced TORC1 activation assay. The kinetics of changes in the steady-state relative molar levels of glycolytic metabolites in wild-type and *gtr1Δ* cells upon glucose addition were indistinguishable (Figure 1A). Notably, the TORC1 activation peak in *gtr1Δ* cells was delayed by about 10 min in comparison with wild-type cells (Figure 1B; quantification in Table S2). These results suggest that delayed TORC1 activation in *gtr1*Δ cells is unlikely to be due to a reduced rate of glycolysis.

To investigate whether metabolism of glucose is required for TORC1 activation, we compared the ability of glucose to activate TORC1 in wild-type and hexokinase-deficient triple mutant (*hxk1Δ hxk2Δ glk1Δ*) cells. Addition of glucose resulted in rapamycin-sensitive Sch9 phosphorylation in wild-type cells but not in hexokinase-deficient cells (Figure 1C; quantification in Table S2), suggesting that phosphorylation of glucose to G6P is essential for glucose-induced TORC1 activation. To confirm this result, we tested the ability of two glucose analogs, 2-deoxyglucose (2-DG) and 6-deoxyglucose (6-DG) to activate TORC1. 6-DG cannot be phosphorylated by hexokinase and is therefore not metabolized (Figure 1D). On the other hand, 2-DG can be phosphorylated by hexokinase, forming 2-DG 6-phosphate, but cannot be metabolized further (Figure 1D). We observed that 2% 2-DG (but not 2% 6-DG) activated TORC1, albeit weakly compared with 2% glucose (Figure S1A; quantification in Table S3). Because 2-DG is a potent inhibitor

CellPress
OPEN ACCESS

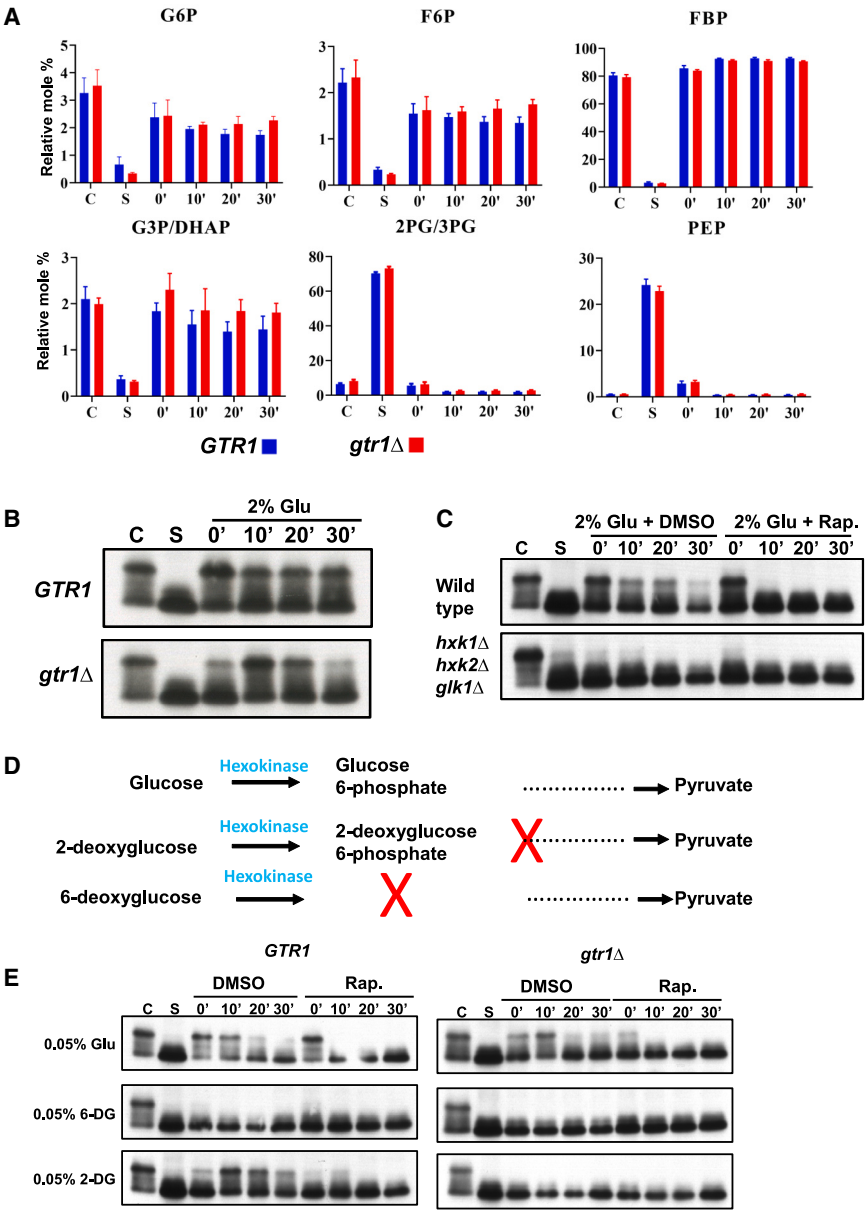

Figure 1. Phosphorylation of glucose is required for glucose-induced TORC1 activation

(A) Wild-type and *gtr1Δ* cells were grown in SC(Synthetic Complete)-glucose (Glu) medium in logarithmic phase (C) and then subjected to complete nutrient starvation by incubating them in water for 1 h. Starved cells (S) were transferred to a solution containing 2% Glu. Aliquots of the cultures were taken after 0, 10, 20, and 30 min for preparing protein extracts and extracting metabolites for LC-MS analysis. Relative molar levels of various glycolytic metabolites in wild-type and *gtr1Δ* cells at different stages of Glu -induced TORC1 activation assay are shown. Error bars indicate standard deviation from 3 biological replicates (n = 3).

(B) Sch9 phosphorylation in wild-type and *gtr1Δ* cells described in (A) was assayed by western blotting.

(C) Wild-type cells and HK-deficient triple mutant cells were grown to logarithmic phase (C) in SC-Raf/Gal medium (2% raffinose and 2% galactose) and subjected to complete nutrient starvation by incubating them in water for 1 h. Starved cells (S) were then transferred to a solution containing 2% Glu in the presence and absence of rapamycin (2 μM). Aliquots of the cultures were taken after 0, 10, 20, and 30 min and used for preparing protein extracts. Phosphorylation of Sch9 was monitored by western blotting.

(D) Schematic showing the metabolic fates of Glu, 2-DG, and 6-DG.

(E) Wild-type cells and *gtr1Δ* cells in logarithmic phase (C) in SC-Glu medium were subjected to complete nutrient starvation by incubating them in water for 1 h. Starved cells (S) were then transferred to a solution containing 0.05% Glu, 0.05% 2-DG, or 0.05% 6-DG in the presence and absence of rapamycin (2 μM). Aliquots of the cultures were taken after 0, 10, 20, and 30 min and used for preparing protein extracts. Phosphorylation of Sch9 was monitored by western blotting.

(A–C and E) Data are representative of 3 independent experiments.

of glycolysis and depletes cellular ATP levels,[23] we tested lower amounts of 2-DG (ranging from 0.2% to 0.0125%) in the TORC1 activation assay. We found that 0.05% 2-DG was most effective in activating TORC1 (Figure S1B; quantification in Table S3). We compared the abilities of 0.05% of 2-DG, 6-DG, and glucose to activate TORC1. Addition of 0.05% glucose or 0.05% 2-DG to starved cells resulted in increased Sch9 phosphorylation that was abolished by rapamycin treatment (Figure 1E; quantification in Table S2). The peak of TORC1 activation by 2-DG was delayed by about 10 min compared with glucose. However, 6-DG failed to activate TORC1 (Figures 1E and S1A; quantification in Tables S2 and S3). These results indicate that hexokinase-mediated conversion of glucose to G6P is essential for TORC1 activation.

We then compared the ability of 0.05% glucose and 2-DG to activate TORC1 in *gtr1Δ* cells. Interestingly, 0.05% glucose, but not 0.05% 2-DG, was able to activate TORC1 in *gtr1Δ* cells (Figure 1E; quantification in Table S2). Because 2-DG cannot proceed beyond the first step in glycolysis, our results imply that metabolism of glucose beyond G6P is required for TORC1 activation via the Rag GTPase-independent pathway. On the other hand, conversion of glucose to G6P is sufficient for the Rag GTPase-dependent pathway for TORC1 activation.

G6P can be catabolized via either the glycolytic pathway or the pentose phosphate pathway (PPP). G6P can also be anabolized, leading to synthesis of trehalose and glycogen. To test which catabolic pathway is required for Rag GTPase-independent TORC1 activation by glucose, we deleted *ZWF1* (which encodes the glucose-6-phosphate dehydrogenase that catalyzes the first committed step in the PPP) or *PFK1/2* (which encode subunits

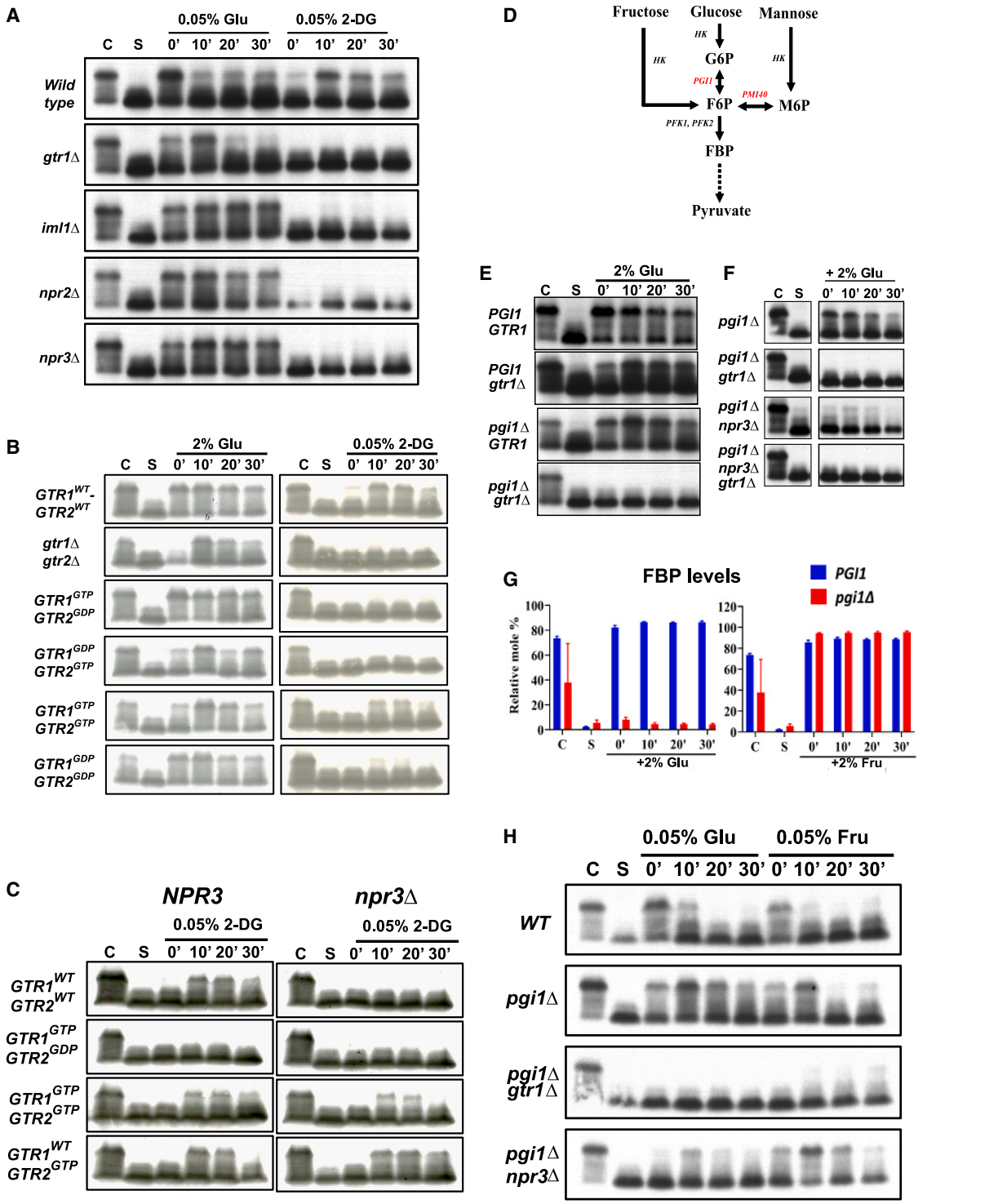

Figure 2. G6P activates the non-canonical pathway of TORC1 activation via $Gtr1^{GTP}/Gtr2^{GTP}$

(A) Wild-type, *gtr1Δ*, *iml1Δ*, *npr2Δ*, and *npr3Δ* cells were grown in logarithmic phase (C) in SC-Glu medium and subjected to complete nutrient starvation by incubating them in water for 1 h. Starved cells (S) were then transferred to a solution containing 0.05% Glu or 0.05% 2-DG. Aliquots of the cultures were taken after 0, 10, 20, and 30 min and used for preparing protein extracts. Phosphorylation of Sch9 was monitored by western blotting.

(B) *gtr1Δ gtr2Δ* cells expressing different combinations of Gtr1/Gtr2 variants (wild type, GTP, GDP, or empty vector) from the tetracycline-inducible promoter were grown to logarithmic phase (C) in SC-Glu medium + tetracycline medium and subjected to complete nutrient starvation by incubating them in water for 1 h.

(legend continued on next page)

of phosphofructokinase, which catalyzes the first committed step in glycolysis). Deletion of *ZWF1* had no major effect on glucose-induced TORC1 activation in wild-type and *gtr1*Δ strains (Figure S2A; quantification in Table S3), indicating that the PPP is not essential for glucose-induced TORC1 activation. However, deletion of *PFK1* or *PFK2* greatly reduced glucose-induced TORC1 activation in the *GTR1* strain (Figures S2B and S2C; quantification in Table S3) and completely abolished TORC1 activation in the *gtr1Δ* strain (Figures S2B and S2C; quantification in Table S3). These results suggest that glycolysis is required for the Rag GTPase-independent pathway for glucose-induced TORC1 activation. This is consistent with the failure of 2-DG to activate TORC1 in *gtr1*Δ cells. Although not essential, glycolysis is also required for efficient glucose-induced TORC1 activation via the Rag GTPase-dependent pathway.

Use of SEACIT mutants uncovers two pathways of Rag GTPase-dependent TORC1 activation by glucose

To confirm the function of Gtr1 in glucose-induced TORC1 activation pathways, we tested the role of the SEACIT complex in TORC1 activation. The SEACIT complex is composed of Iml1/Npr2/Npr3 and inhibits TORC1 by promoting hydrolysis of GTP bound to Gtr1. We tested the ability of glucose and 2-DG to activate TORC1 in wild-type and *iml1Δ/npr2Δ/npr3Δ* strains that are deficient in SEACIT function. As expected, glucose-induced TORC1 activation was stabilized in SEACIT mutants in comparison with the wild-type strain (Figure 2A; quantification in Table S2). Deletion of *GTR1* abolished the stabilizing effect of SEACIT mutations on TORC1 activation (Figure S3A; quantification in Table S3). These results support the notion that stabilization of $Gtr1^{GTP}$ in SEACIT-deficient mutants boosts TORC1 activation. Much to our surprise, we found that 2-DG-induced activation of TORC1 was abolished in SEACIT mutant strains (Figures 2A and S3A; quantification in Tables S2 and S3). Although the $Gtr1^{GTP}$ form boosts glucose-induced TORC1 activation, it is deficient in 2-DG-induced TORC1 activation. To confirm this result, we constructed *gtr1Δ gtr2Δ* strains expressing either wild-type Gtr1/Gtr2 or various mutant heterodimers that bind GTP or GDP ($Gtr1^{GTP}$-$Gtr2^{GDP}$, $Gtr1^{GDP}$- $Gtr2^{GTP}$, $Gtr1^{GTP}$- $Gtr2^{GTP}$, $Gtr1^{GDP}$- $Gtr2^{GDP}$). We used *gtr1Δ gtr2Δ* strains containing an empty vector as a negative control. As expected, the canonical active form $Gtr1^{GTP}$- $Gtr2^{GDP}$ stabilized glucose-induced TORC1 activation in comparison with cells expressing wild-type Gtr1/Gtr2 (Figure 2B; quantification in Table S2). In strains expressing the inactive form $Gtr1^{GDP}$-$Gtr2^{GTP}$, glucose-induced TORC1 activation was delayed, as observed in *gtr1Δ gtr2Δ* cells. Consistent with our results with SEACIT mutants, 2-DG failed to activate TORC1 in the $Gtr1^{GTP}$-$Gtr2^{GDP}$-expressing strain (Figure 2B; quantification in Table S2). Remarkably, 2-DG activated TORC1 in cells expressing $Gtr1^{GTP}$- $Gtr2^{GTP}$ (Figure 2B; quantification in Table S2). These results indicate that glucose activates TORC1 through Gtr1/Gtr2 via at least two pathways. In the first pathway, $Gtr1^{GTP}$ -$Gtr2^{GDP}$ activates TORC1 upon glucose addition, and we refer to this as the canonical pathway. This pathway requires metabolism beyond G6P as 2-DG fails to stimulate this. In the second pathway, 2-DG activates TORC1, possibly via $Gtr1^{GTP}$-$Gtr2^{GTP}$, and we refer to as the ''non-canonical pathway'' for the remainder of this manuscript.

Addition of 2-DG failed to activate TORC1 in *npr3Δ* cells, which is predicted to be enriched for the $Gtr1^{GTP}$ form. This appears to be inconsistent with the notion that the $Gtr1^{GTP}$- $Gtr2^{GTP}$ heterodimer activates TORC1 via the non-canonical pathway. We hypothesized that blocking hydrolysis of GTP bound to Gtr1 could either prevent GTP binding to Gtr2 or block dissociation of GDP from Gtr2. This will prevent the formation of $Gtr1^{GTP}$-$Gtr2^{GTP}$ heterodimers in *npr3Δ* cells and block 2-DG-induced TORC1 activation. If this hypothesis is true, then expression of the $Gtr2^{GTP}$ mutant should suppress *npr3Δ*'s defect in 2-DG-induced TORC1 activation. We compared 2-DG-induced TORC1 activation in *npr3Δ GTR2* and *npr3Δ* $GTR2^{GTP}$ cells (Figure 2C; quantification in Table S2). 2-DG activated TORC1 in *npr3Δ* $GTR2^{GTP}$ cells but not in *npr3Δ GTR2* cells, supporting the idea that $Gtr1^{GTP}$-$Gtr2^{GTP}$ activates TORC1 via the non-canonical pathway (Figure 2C; quantification in Table S2). Lst4 is required for hydrolysis of GTP bound to Gtr2.[24] We found that 2-DG-mediated TORC1 activation was quicker in *lst4Δ* cells compared with wild-type cells, further supporting the idea that the $Gtr1^{GTP}$-$Gtr2^{GTP}$ heterodimer activates TORC1 via the non-canonical pathway (Figure S3B; quantification in Table S3).

G6P activates TORC1 via a non-canonical Rag GTPase-dependent pathway

Because 2-DG is a synthetic compound, the non-canonical pathway of TORC1 activation observed could be an artifact. If 2-DG induced TORC1 activation is physiological, then G6P

Starved cells (S) were then transferred to a solution containing 0.05% Glu or 0.05% 2-DG. Aliquots of the cultures were taken after 0, 10, 20, and 30 min and used for preparing protein extracts. Phosphorylation of Sch9 was monitored by western blotting.

(C) Wild-type and *npr3Δ* cells expressing different combinations of Gtr1/Gtr2 variants ($Gtr1^{WT}$-$Gtr2^{WT}$, $Gtr1^{GTP}$- $Gtr2^{GDP}$, $Gtr1^{GTP}$-$Gtr2^{GTP}$, and $Gtr1^{WT}$-$Gtr2^{GTP}$) from the tetracycline-inducible promoter were treated with either 0.05% Glu or 0.05% 2-DG in the TORC1 activation assay and analyzed as described in (B).

(D) Fructose and mannose but not glucose can enter glycolysis without phosphoglucoisomerase.

(E) Wild-type, *gtr1Δ*, *pgi1Δ*, and *pgi1Δ gtr1Δ* cells were grown to logarithmic phase (C) in SC-Raf/Gal medium and subjected to complete nutrient starvation by incubating them in water for 1 h. Starved cells (S) were then transferred to a solution containing 2% Glu. Aliquots of the cultures taken after 0, 10, 20, and 30 were used for preparing protein extracts. Phosphorylation of Sch9 was monitored by western blotting.

(F) *pgi1Δ*, *pgi1Δ gtr1Δ*, *pgi1Δ npr3Δ*, and *pgi1Δ npr3Δ gtr1Δ* cells were tested in the Glu-induced TORC1 activation assay as described in (E).

(G) Wild-type and *pgi1Δ* cells were grown in SC-Raf/Gal medium in logarithmic phase (C) and then subjected to complete nutrient starvation by incubating them in water for 1 h. Starved cells (S) were transferred to a solution containing 2% Glu or 2% fructose. Aliquots of the cultures were taken after 0, 10, 20, and 30 min for preparing protein extracts and for extracting metabolites for LC-MS analysis. The percentage mole fraction of FBP levels is plotted for wild-type and *pgi1Δ* cells treated with 2% Glu (left) or 2% fructose (right) at the indicated time points. Error bars indicate standard deviation from 3 biological replicates (n = 3).

(H) Wild-type, *pgi1Δ*, *pgi1Δ gtr1Δ*, and *pgi1Δ npr3Δ* cells were tested with 0.05% Glu and 0.05% fructose in the TORC1 activation assay as described in (E).

(A–C and E–H) Data are representative of 3 independent experiments.

should also activate TORC1 via the non-canonical pathway. To test this, we constructed a phosphoglucoisomerase deletion strain (*pgi1Δ*) that cannot interconvert G6P and F6P (Figure 2D). Addition of glucose to *pgi1Δ* cells is expected to cause an accumulation of G6P, thus "phenocopying" 2-DG-treated cells. Addition of glucose activated TORC1 in *pgi1Δ* cells but not in *pgi1Δ gtr1Δ* cells (Figures 2E and 2F; quantification in Table S2). This is consistent with our observations that 2-DG-induced TORC1 activation is dependent on Gtr1. Crucially, addition of glucose to *pgi1Δ npr3Δ* cells resulted in drastically reduced TORC1 activation in comparison with *pgi1Δ* cells (Figure 2F; quantification in Table S2). Our results support the notion that G6P formation activates TORC1 via a Rag GTPase-dependent non-canonical pathway. Conversely, because activation by glucose (but not by 2-DG) is stabilized in SEACIT mutants in comparison with wild-type cells, we can conclude that glucose has to be metabolized beyond G6P for TORC1 activation via the Rag GTPase-dependent canonical pathway.

Fructose is phosphorylated by hexokinase to form F6P and can enter glycolysis without phosphoglucoisomerase activity (Figure 2D). We confirmed this by assaying changes in the levels of glycolytic metabolites caused by addition of fructose and glucose to *pgi1Δ* strains. Addition of fructose but not glucose to the *pgi1Δ* strain increased the relative molar levels of FBP (Figure 2G). By titrating the amount of fructose, we found that 0.05% fructose was optimal for activating TORC1 in the *pgi1Δ* strain (data not shown). TORC1 activation induced by 0.05% fructose was more stable in the *pgi1Δ npr3Δ* strain in comparison with the *pgi1Δ* strain (Figure 2H; quantification in Table S2). In contrast, activation by 0.05% glucose was reduced by about 3.1-fold in *pgi1Δ npr3Δ* cells in comparison with *pgi1Δ* cells (Figure 2H; quantification in Table S2). These results support the notion that metabolism to G6P activates TORC1 through a non-canonical pathway, and metabolism beyond G6P is required for the Rag GTPase-dependent canonical pathway for TORC1 activation.

Intriguingly, addition of 2% fructose (unlike 0.05% fructose) to starved *pgi1Δ* cells did not activate TORC1. One possibility is that the ATP levels in *pgi1Δ* strain could be low and further depleted by addition of 2% fructose (ATP consumed for FBP formation). We measured ATP levels in wild-type and *pgi1Δ* cells treated with 0.05% fructose and 2% fructose following starvation. In both wild-type and *pgi1Δ* cells, ATP levels decreased for the first 10 min following addition of fructose and then increased in the subsequent 20 min (Figure S4A). ATP levels in 0.05% fructose-treated *pgi1Δ* cells were higher than in 2% fructose-treated *pgi1Δ* cells at 0 and 10 min (Figure S4A), which coincides with the timing of TORC1 activation in 0.05% fructose-treated *pgi1Δ* cells (Figure 2H). While reduced ATP levels in 2% fructose-treated *pgi1Δ* cells might explain the lack of TORC1 activation, it is possible that there are other consequences of 2% fructose addition that impair TORC1 activation in *pgi1Δ* cells.

Like fructose, mannose can enter glycolysis without phosphoglucose isomerase activity (Figure 2D). Hence, mannose should also activate TORC1 in the *pgi1Δ gtr1Δ* strain like fructose. Indeed, 0.05% mannose (but not 2% mannose) activated TORC1 in the *pgi1Δgtr1Δ* strain like fructose (Figure S4B; quantification in Table S3).

We then tested whether mannose 6-phosphate (M6P) can also activate the non-canonical Rag GTPase-dependent pathway. Mannose is phosphorylated by hexokinase to form M6P, which is then converted into F6P by the phosphomannose isomerase Pmi40. We compared the kinetics of TORC1 activation induced by glucose and mannose (2% and 0.05%) in wild-type, *gtr1Δ*, *pmi40Δ*, and *pmi40Δ gtr1Δ* cells. As expected, glucose-induced TORC1 activation was comparable in wild-type, *pmi40Δ*, and their *gtr1Δ* variants (Figure S4C; quantification in Table S3). Mannose and glucose activated TORC1 to comparable extents in wild-type and *gtr1Δ* cells. Interestingly, 0.05% mannose, but not 2% mannose, activated TORC1 in *pmi40Δ* cells. TORC1 activation induced by 0.05% mannose was abolished in *pmi40Δ gtr1Δ* cells (Figure S4C; quantification in Table S3). Taken together, our results with *pgi1Δ* and *pmi40Δ* cells indicate that formation of G6P/M6P is necessary and sufficient to activate the Rag GTPase-dependent non-canonical pathway. Activation of TORC1 by mannose in the *pgi1Δgtr1Δ* strain (Figure S4C; quantification in Table S3), but not in the *pmi40Δ gtr1Δ* strain (Figure S4C; quantification in Table S3), further supports the notion that glycolysis beyond M6P is required for the Rag GTPase-independent pathway of TORC1 activation.

TORC1 activation data with 2%/0.05% mannose in *pmi40Δ* cells is reminiscent of our results with wild-type cells treated with 2%/0.05% 2-DG (Figures S1A and S1B). Treatment of *pmi40Δ* cells with 2% mannose or treatment of wild-type cells with 2% 2-DG is expected to cause an accumulation of high concentrations of M6P or its analog 2-DG 6-phosphate, respectively. We measured ATP levels in starved wild-type and *pmi40Δ* cells treated with 0.05% mannose and 2% mannose. In wild-type cells treated with 2% mannose, ATP levels decreased for the first 10 min and then increased in the subsequent 20 min (Figure S4D). In contrast, ATP levels in 2% mannose-treated *pmi40Δ* cells decreased over the course of 30 min. ATP levels in 0.05% mannose-treated *pmi40Δ* cells at 10 and 20 min were higher than in 2% mannose-treated *pmi40Δ* cells (Figure S4D), which coincides with the timing of TORC1 activation in 0.05% mannose-treated *pgi1Δ* cells (Figure S4C). These results are suggestive of a link between ATP levels and TORC1 activation in mannose-treated *pmi40Δ* cells. Alternatively, high concentrations of M6P (and 2-DG 6-phosphate) might inhibit TORC1 activation.

Formation of FBP is sufficient for the canonical Rag GTPase-dependent pathway of TORC1 activation

We then sought to identify glycolytic steps downstream of G6P that are required for the Rag GTPase-dependent canonical pathway and the Rag GTPase-independent pathway of TORC1 activation. As mentioned above, inactivating phosphofructokinase (Pfk1/Pfk2), which converts F6P to FBP, severely affected glucose-induced TORC1 activation. To test whether the poor TORC1 activation observed in *pfk2Δ* cells was via the canonical pathway, we tested the effect of *npr3*Δ on TORC1 activation in *pfk2* cells. While TORC1 activation was stabilized in *npr3Δ* cells, TORC1 activation was abolished in *pfk2Δ npr3Δ* cells (Figure S2C; quantification in Table S3), suggesting that the weak activation in *pfk2*Δ cells was via the non-canonical pathway. These results also indicated that glycolytic reactions

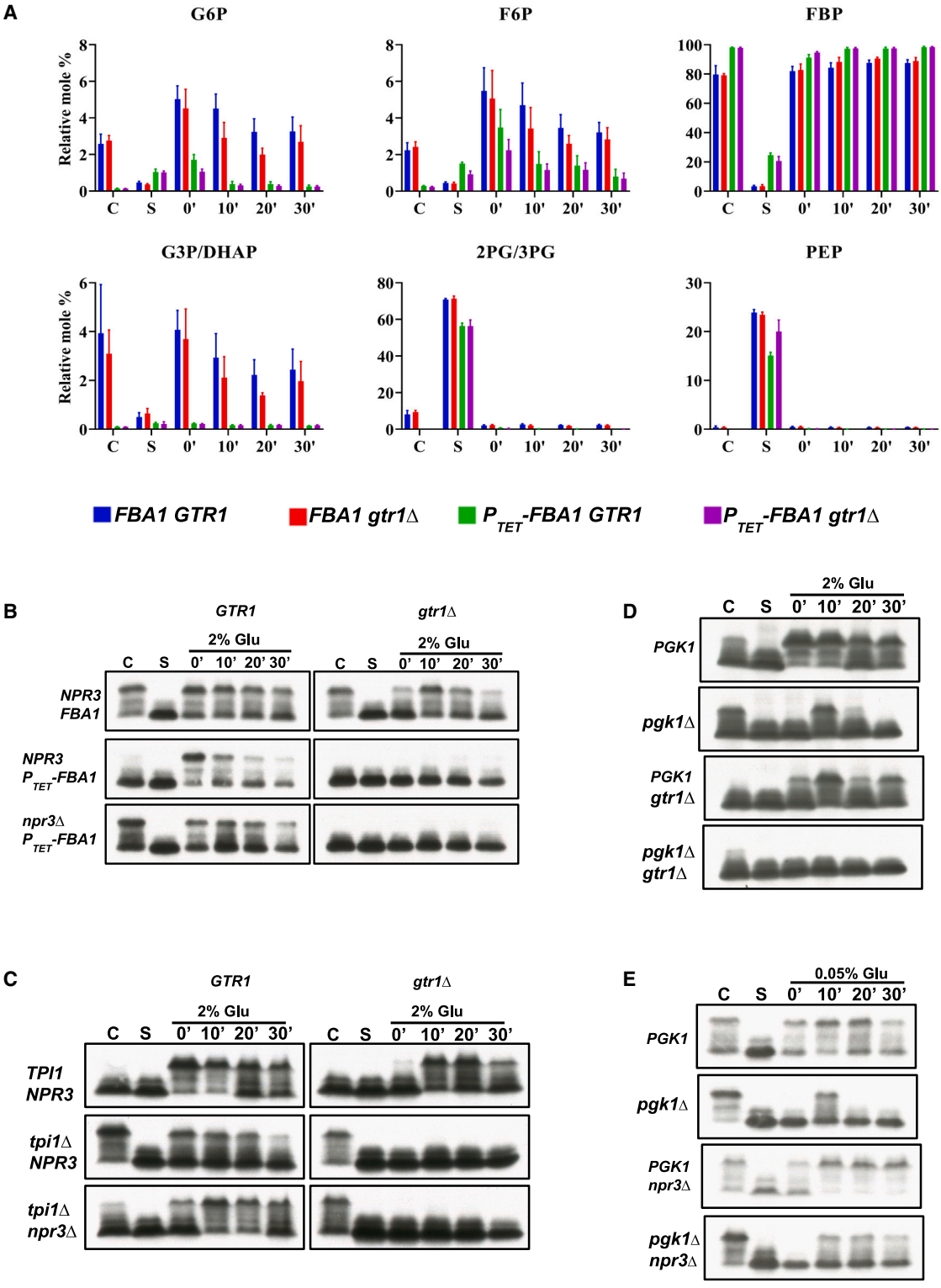

Figure 3. Formation of FBP from Glu is sufficient for the canonical pathway of TORC1 activation

(A) Wild-type and P_{Tetoff}-*FBA1* cells were grown in SC-Glu medium in the presence of tetracycline and then subjected to complete nutrient starvation by incubating them in water for 1 h. Starved cells (S) were transferred to a solution containing 2% Glu. Aliquots of the cultures were taken after 0, 10, 20, and 30 min for extracting metabolites for LC-MS analysis and for preparing protein extracts. Relative molar levels of various glycolytic metabolites in wild-type and P_{Tetoff}-*FBA1* cells at different stages of Glu-induced TORC1 activation assay are shown. Error bars indicate standard deviation from 3 biological replicates (n = 3).

(legend continued on next page)

downstream of F6P are required for the canonical pathway of TORC1 activation.

Aldolase (Fba1) catalyzes the conversion of FBP into G3P and DHAP. Because *FBA1* is an essential gene, we constructed a yeast strain that expresses *FBA1* from the tetracycline-repressible promoter. P_{Tetoff}-*FBA1* cells were dead on tetracycline-containing SC-glucose medium plates (data not shown). To deplete aldolase, P_{Tetoff}-*FBA1* cells were grown overnight in synthetic medium in the presence of tetracycline. Cells from the overnight culture were inoculated at an optical density 600 (OD_{600}) of 0.2 and cultured further for 5–6 h in SC-glucose medium + tetracycline. A strain expressing *FBA1* from the native promoter served as a control. Growth of P_{Tetoff}-*FBA1* cells was severely inhibited in the presence of tetracycline, indicating efficient depletion. We compared the relative proportions of glycolytic metabolites in wild-type and *FBA1*-depleted cells following addition of glucose. Relative molar levels of FBP following glucose addition increased to 92% in wild-type cells but increased to 97% in the P_{Tetoff}-*FBA1* cells (Figure 3A). Crucially, the downstream glycolytic metabolites (G3P/DHAP) were not detectable in P_{Tetoff}-*FBA1* cells, indicating efficient depletion of *FBA1* (Figure 3A). TORC1 was activated by glucose, albeit at reduced levels, in P_{Tetoff}-*FBA1* cells in comparison with wild-type cells (Figure 3B; quantification in Table S2). In contrast, TORC1 activation was completely blocked in P_{Tetoff}-*FBA1 gtr1Δ* cells (Figure 3B; quantification in Table S2), indicating that metabolism of glucose beyond FBP is required for TORC1 activation via the Rag GTPase-independent pathway. However, formation of FBP is sufficient for the Rag GTPase-dependent pathway of TORC1 activation. To confirm that the activation of TORC1 by glucose in P_{Tetoff}-*FBA1* strain was via the canonical pathway, we compared glucose-induced TORC1 activation in P_{Tetoff}-*FBA1* and P_{Tetoff}-*FBA1 npr3Δ* cells. TORC1 was activated following addition of glucose and remained stable in P_{Tetoff}-*FBA1 npr3Δ* cells in comparison with P_{Tetoff}-*FBA1* cells (Figure 3B; quantification in Table S2). Taken together, our results suggest that formation of FBP is sufficient for TORC1 activation via the canonical pathway but that further glycolytic steps beyond FBP formation are required for the Rag GTPase-independent pathway of TORC1 activation.

Complete glycolysis is essential for TORC1 activation via the Rag GTPase-independent pathway

To determine glycolytic steps downstream of FBP formation that are required for the Rag GTPase-independent pathway of TORC1 activation, we first tested the role of triosephosphate isomerase (Tpi1), which interconverts DHAP and G3P. In *tpi1Δ* cells, G3P but not DHAP generated by fructose1,6-bisphosphate aldolase will be metabolized further in glycolysis. We analyzed the relative levels of glycolytic metabolites in wild-type and *tpi1Δ* cells during the glucose-induced TORC1 activation assay. As expected, levels of DHAP in *tpi1Δ* cells (cycling and starved) were elevated in comparison with wild-type cells (Figure S5). Addition of glucose to starved *tpi1Δ* cells caused a rise in relative FBP levels, albeit to a lower extent than in wild-type cells (Figure S5A). TORC1 activation in *tpi1Δ* cells was reduced by about 2-fold in comparison with wild-type cells (Figure 3C; quantification in Table S2). However, TORC1 activation was completely abolished in *tpi1Δ gtr1Δ* cells (Figure 3C). *tpi1Δ* cells are expected to undergo complete glycolysis without generating net ATP because one molecule of DHAP is unutilized. Consistent with this prediction, we observed that ATP levels increased following glucose addition to starved wild-type and *gtr1Δ* cells but not in *tpi1Δ* and *tpi1Δ gtr1Δ* cells (Figure S5B). These results suggest that net ATP production from glycolysis is required for the Rag GTPase-independent pathway of TORC1 activation. To confirm that activation of TORC1 by glucose in *tpi1Δ* cells is via the Rag GTPase-dependent canonical pathway, we compared TORC1 activation in *tpi1Δ* and *tpi1Δ npr3Δ* cells. Glucose-induced TORC1 activation was more stable in *tpi1Δ npr3Δ* cells in comparison with *tpi1Δ* cells, indicating that triosephosphate isomerase activity is not required for TORC1 activation by glucose via the Rag GTPase-dependent canonical pathway (Figure 3C; quantification in Table S2). These results further support the notion that formation of FBP is sufficient for activation of TORC1 via the canonical Rag GTPase-dependent pathway.

We then examined the ability of *pgk1Δ*, *gpm1Δ*, and *cdc19Δ* mutants that are defective in the remaining glycolytic steps to metabolize glucose under our TORC1 assay conditions. Relative molar levels of G6P/F6P/FBP in *cdc19Δ* and *gpm1Δ* cells did not increase following addition of 2% glucose, indicating that the *cdc19Δ* and *gpm1Δ* mutant cells were poor in initiating glycolysis (Figure S6A). Addition of glucose to *cdc19Δ* and *gpm1Δ* cells failed to activate TORC1, consistent with the idea that glycolysis is essential for glucose-induced TORC1 activation (Figure S6B; quantification in Table S3). Interestingly, we observed an accumulation of FBP in starved *pgk1Δ* cells and a further increase in FBP levels upon glucose addition (Figure S6A). Glucose (2%) activated TORC1 in wild-type and *pgk1Δ* cells (Figure 3D; quantification in Table S2). However, glucose failed to activate TORC1 in *pgk1Δ gtr1Δ* cells (Figure 3D). To test whether the canonical pathway is active in *pgk1Δ* cells, we compared glucose-induced TORC1 activation

(B) Sch9 phosphorylation in wild-type and P_{Tetoff}-*FBA1* cells was assayed by western blotting.

(C) Wild-type and *tpi1Δ* cells were grown in SC-EtOH/Gly medium (2% ethanol and 2% glycerol) and then subjected to complete nutrient starvation by incubating them in water for 1 h. Starved cells (S) were transferred to a solution containing 2% Glu. Aliquots of the cultures were taken after 0, 10, 20, and 30 min for analysis for Sch9 phosphorylation and for extracting metabolites for LC-MS analysis. Sch9 phosphorylation in wild-type and *tpi1Δ* cells was assayed by western blotting. Relative molar levels of various glycolytic metabolites in wild-type and *tpi1Δ* cells at different stages of Glu -induced TORC1 activation assay are shown in Figure S5.

(D) Wild-type and *pgk1Δ* cells were treated as in (C), and Sch9 phosphorylation was assayed by western blotting. Relative molar levels of various glycolytic metabolites in wild-type and *pgk1Δ* cells at different stages of Glu-induced TORC1 activation assay are shown in Figure S6.

(E) Wild-type, *pgk1Δ*, *npr3Δ*, and *pgk1Δ npr3Δ* cells were analyzed in the TORC1 activation assay as described in (D). Sch9 phosphorylation was assayed by western blotting.

All data are representative of 3 independent experiments.

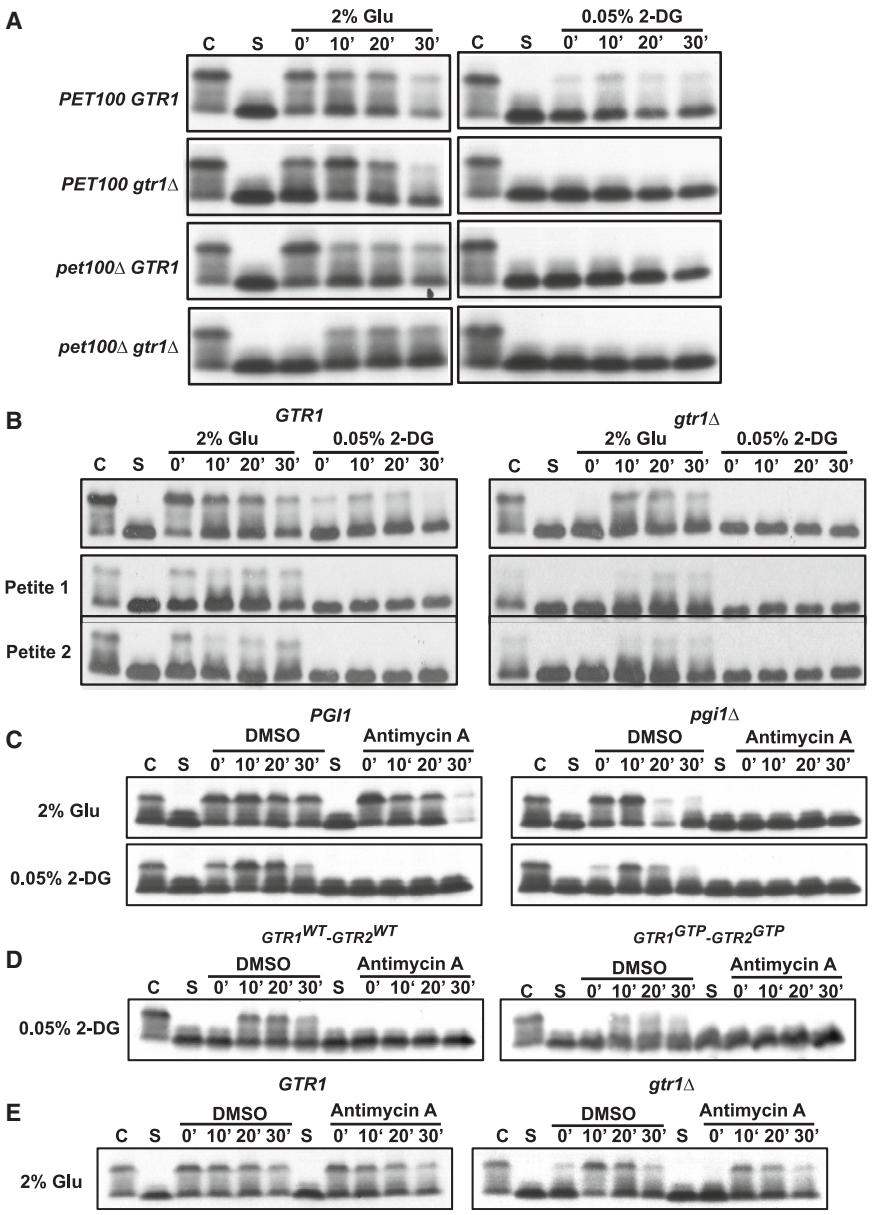

Figure 4. Mitochondrial function is required for the non-canonical pathway of Glu-induced TORC1 activation

(A) Wild-type, *gtr1Δ*, *pet100Δ*, and *pet100Δ gtr1Δ* cells grown to logarithmic phase (C) in SC-Glu medium were subjected to complete nutrient starvation by incubating them in water for 1 h. Starved cells (S) were then transferred to a solution containing 2% Glu or 0.05% 2-DG. Aliquots of the cultures were taken after 0, 10, 20, and 30 min and used for preparing protein extracts. Phosphorylation of Sch9 was monitored by western blotting.

(B) Same as described in (A) but performed with wild-type and *gtr1Δ* cells and two petite strains with or without *gtr1Δ*.

(C) Same as described in (A) but performed with wild-type and *pgi1Δ* cells with or without antimycin treatment (50 μM).

(D) Same as described in (A) but performed with 2-DG-treated cells expressing either $Gtr1^{WT}$-$Gtr2^{WT}$ or $Gtr1^{GTP}$-$Gtr2^{GTP}$ with or without antimycin treatment (50 μM).

(E) Same as described in (A) but performed with wild-type and *gtr1Δ* cells with or without antimycin treatment (50 μM) and treated with 2% Glu.

All data are representative of 3 independent experiments.

in *pgk1Δ* and *pgk1Δ npr3Δ* cells. We used lower concentrations of glucose (0.05%) because we reasoned that *pgk1Δ* cells might have lower amounts of ATP. TORC1 activation was stabilized in *pgk1Δ npr3Δ* cells in comparison with *pgk1Δ* cells, indicating that phosphoglycerate kinase activity is not required for the canonical pathway for glucose-induced TORC1 activation (Figure 3E; quantification in Table S2). These results further support the idea that conversion of glucose to FBP is sufficient for TORC1 activation via the canonical Rag GTPase-dependent pathway but that complete glycolysis of glucose is required for the Rag GTPase-independent pathway. It is notable that starved *pgk1Δ* cells contain FBP but lack TORC1 activity. This indicates that the presence of FBP is not sufficient for TORC1 activation.

Mitochondrial function is essential for the non-canonical pathway of TORC1 activation

Following glycolysis, pyruvate is converted into acetyl-coenzyme A (CoA), which generates ATP via the mitochondrial oxidative phosphorylation pathway. We tested whether mitochondrial function is required for glucose-induced TORC1 activation. We generated the *pet100Δ* strain, which lacks mitochondrial electron transport chain function, and petite strains by ethidium bromide treatment of wild-type cells. Both the *pet100Δ* and petite strains were unable to grow in medium containing a non-fermentable carbon source (data not shown), consistent with a defect in mitochondrial function. We compared the ability of 2-DG and glucose to activate TORC1 in the wild type, *pet100Δ*, and their *gtr1Δ* variants. Glucose-induced TORC1 activation in the wild-type and *pet100Δ* strains was comparable. TORC1 activation in *pet100Δ gtr1Δ* was delayed by about 10 min relative to the *gtr1Δ* strain (Figure 4A; quantification in Table S2). However, 2-DG failed to activate TORC1 in *pet100Δ* strains (Figure 4A; quantification in Table S2). Glucose-induced TORC1 activation in petite strains was weaker compared with the wild-type strain (Figure 4B; quantification in Table S2), but the relative timing of TORC1 activation in wild-type and *gtr1Δ* petite strains was comparable with their wild type counterparts. However, 2-DG failed to activate TORC1 in the petite strains (Figure 4B; quantification in

Table S2). Inactivation of the SEACIT complex stabilized TORC1 activity in glucose-treated *pet100Δ* cells (Figure S7A; quantification in Table S3)). These results indicate that a functional mitochondrion is essential for the non-canonical pathway but not required for the canonical Rag GTPase-dependent and Rag GTPase-independent pathways. To confirm this, we tested the effect of antimycin A, an inhibitor of the mitochondrial respiratory chain,[25] on the non-canonical pathway of TORC1 activation. We compared the ability of glucose and 2-DG to activate TORC1 in wild-type and *pgi1Δ* cells in the presence or absence of antimycin A treatment. TORC1 activation in 2% glucose-treated wild-type cells was unaffected by antimycin A treatment (Figure 4C; quantification in Table S2). In contrast, TORC1 activation in 2% glucose-treated *pgi1Δ* cells was completely abolished by antimycin A treatment. Importantly, 0.05% 2-DG-induced TORC1 activation in both wild-type and *pgi1Δ* cells was blocked by antimycin A treatment (Figure 4C; quantification in Table S2). In addition, 2-DG-induced TORC1 activation in cells expressing $Gtr1^{GTP}$-$Gtr2^{GTP}$ was also inhibited by antimycin A treatment (Figure 4D; quantification in Table S2). These results demonstrate that the non-canonical pathway of TORC1 activation requires mitochondrial function. We then tested whether mitochondrial function is required for the Rag-GTPase independent pathway by comparing the effect of antimycin A treatment on TORC1 activation in wild-type and *gtr1Δ* cells treated with 2% glucose. While antimycin A treatment had no effect on TORC1 activation in wild-type cells, it modestly reduced (~25%) TORC1 activation in *gtr1Δ* cells (Figure 4E; quantification in Table S2). This result, along with the effect of *pet100Δ* mutation on the Gtr1-independent pathway (Figure 4A), suggests that mitochondrial function is required for efficient activation of the Rag-GTPase-independent pathway. In summary, active mitochondrial function is essential for the non-canonical pathway of TORC1 activation but largely dispensable for the Rag GTPase-dependent canonical/and Rag GTPase-independent pathways of TORC1 activation.

Known FBP-binding proteins are not required for the canonical pathway of TORC1 activation

FBP formation is essential for glucose-induced TORC1 activation via the canonical pathway. FBP could activate TORC1 by directly binding to its subunits or indirectly via proteins that regulate TORC1 activity. Alternatively, generation of FBP from glucose could modify the cellular milieu, which then activates TORC1. We explored the role of three FBP-binding proteins (namely, aldolase, pyruvate kinase, and fructose 1,6-bisphosphatase) in glucose-induced TORC1 activation. FBP binds to aldolase and inactivates AMPK in human cells.[26] To test whether the yeast aldolase has a non-enzymatic role in glucose-induced TORC1 activation, we replaced the yeast aldolase with the human aldolase. Although yeast and human aldolases catalyze the same enzymatic reaction, they are not evolutionarily related and have no detectable sequence homology.[27] Human aldolase rescued the lethal phenotype of yeast *fba1* deletion (data not shown). Glucose induced TORC1 activation in the human aldolase-expressing yeast strain and was comparable with activation in wild-type yeast cells (Figure 5A; quantification in Table S2). Furthermore, TORC1 activation was enhanced in *npr3Δ* $FBA1^{human}$ cells (Figure 5A; quantification in Table S2). These results strongly suggest that aldolase does not have a non-catalytic role in TORC1 activation in yeast. Deletion of the *FBP1* gene, which encodes fructose1,6-bisphosphatase, did not affect glucose induced TORC1 activation (Figure 5B; quantification in Table S2). Moreover, *npr3*Δ stabilized glucose-induced TORC1 activation in *fbp1Δ* cells (Figure 5B; quantification in Table S2), indicating that activation of the canonical pathway does not require fructose 1,6-bisphosphatase.

Enzymatic activity of Cdc19 (pyruvate kinase) is induced upon FBP binding (Figure 5C). To test whether FBP binding to Cdc19 is required for glucose-induced TORC1 activation, we constructed a catalytically active variant of Cdc19 that is deficient in FBP binding. R459 in Cdc19 forms an electrostatic interaction with the 1′-phosphate group of FBP.[28] The R459Q mutation in Cdc19 abolishes FBP binding (Figure 5C).[29] A strain expressing $Cdc19^{R459Q}$ was unable to grow in nutrient medium with glucose as a carbon source, indicating that R459Q inhibits Cdc19's enzymatic activity (data not shown). The E392A mutation in Cdc19 renders the catalytic activity independent of FBP binding.[22,29] We tested whether the E392A mutation could restore the enzymatic activity of the $Cdc19^{R459Q}$ mutant. Indeed, a strain expressing the $Cdc19^{E392A\ R459Q}$ mutant was able to grow in glucose-containing medium (data not shown). TORC1 activation induced by glucose in $Cdc19^{WT}$ and $Cdc19^{E392A\ R459Q}$ strains were comparable (Figure 5C; quantification in Table S2). These results indicate that Cdc19's ability to bind FBP does not have a non-catalytic role in glucose-induced TORC1 activation.

V-ATPase activity is required for the Rag GTPase-independent pathway of TORC1 activation

V-ATPase is a multisubunit complex that uses energy derived from ATP hydrolysis to pump protons into the vacuole and maintains the low pH inside the yeast vacuoles.[30] V-ATPase disassembles during glucose starvation and reassembles upon glucose re-addition in yeast.[30] V-ATPase reassembly in yeast is facilitated by the RAVE (regulator of the ATPase of vacuolar and endosomal membranes) complex composed of Rav1, Rav2, and Skp1.[31,32] To test whether V-ATPase reassembly is required for glucose-induced TORC1 activation, we compared TORC1 activation in wild-type, *gtr1Δ*, *rav2Δ*, and *rav2Δ gtr1Δ* cells. Glucose-induced TORC1 activation in the *rav2Δ* mutant was comparable with the wild-type strain at the onset but decayed rapidly after 20 min (Figure 6A; quantification in Table S2). However, glucose-induced TORC1 activation was severely compromised in *rav2Δ gtr1Δ* cells (Figure 6A; quantification in Table S2). These results suggest that V-ATPase reassembly is required for the Rag-GTPase-independent TORC1 activation pathway. Effect of *rav2Δ* on TORC1 activation in *GTR1* cells is more pronounced at later time points. This could be due to the 10-min delay in activation of TORC1 via the Rag GTPase-independent pathway in comparison with the Rag GTPase-dependent pathway.

To test whether V-ATPase reassembles during the glucose-induced TORC1 activation assay, we tagged the cytosolic (Vph1) and membrane (Vma5) subunits of the V-ATPase with mCherry and GFP, respectively. We tested the effect of two glycolytic mutations, *tpi1Δ* and *pgk1Δ*, on glucose-induced

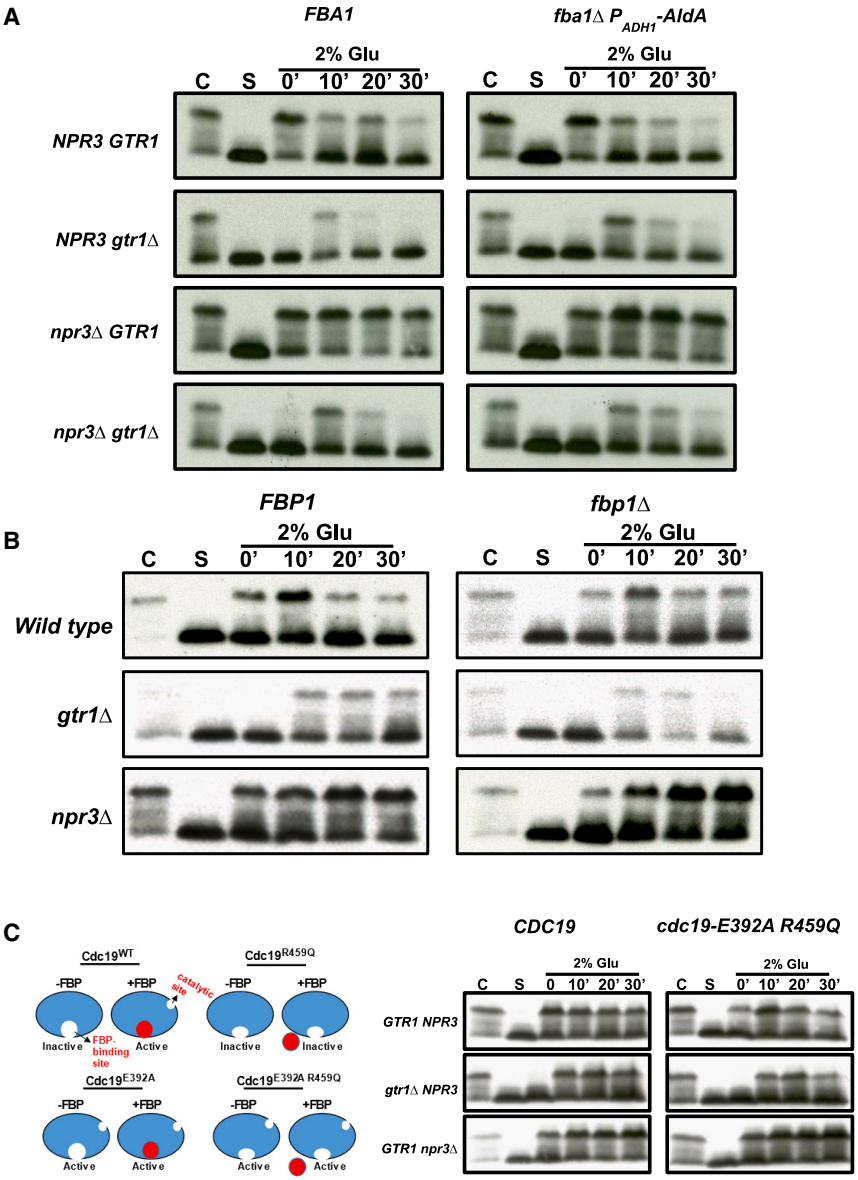

Figure 5. FBP-binding proteins and the canonical pathway

(A) Wild-type, *gtr1Δ*, *npr3Δ*, and *npr3Δgtr1Δ* cells expressing native aldolase or human aldolase A were grown in logarithmic phase (C) in SC-Glu medium and subjected to complete nutrient starvation by incubating them in water for 1 h. Starved cells (S) were then transferred to a solution containing 2% Glu. Aliquots of the cultures were taken after 0, 10, 20, and 30 min and used for preparing protein extracts. Phosphorylation of Sch9 was monitored by western blotting.

(B) Similar to (A) but performed with wild-type, *gtr1Δ*, *npr3Δ*, *fbp1Δ*, *fbp1Δ gtr1Δ*, and *fbp1Δ npr3Δ* cells.

(C) Similar to (A) but performed with wild-type, *npr3Δ*, and *gtr1Δ* cells expressing either $Cdc19^{WT}$ or $Cdc19^{E392A\ R459Q}$. Cartoon on the left shows the effect of FBP (red circle) and mutations (E392A and R459Q) on Cdc19's catalytic/FBP-binding activities

All data are representative of 3 independent experiments.

V-ATPase reassembly. We grew the wild-type, *tpi1Δ* and *pgk1Δ* cells in ethanol-glycerol medium to log phase and then subjected them to complete nutrient starvation for 1 h. We then added glucose (2%) to starved cells and assayed V-ATPase reassembly 15 and 30 min after glucose addition. V-ATPase was disassembled in cells growing in ethanol-glycerol medium (Figure 6B). V-ATPase assembly following glucose addition occurred in wild-type and *tpi1Δ* cells but not in *pgk1Δ* cells. This suggests that complete glycolysis but not ATP generation per se is required for glucose-induced V-ATPase assembly. However, glucose-induced TORC1 activation via the Rag GTPase-independent pathway was defective in both *tpi1Δ* (Figure 3C; quantification in Table S2) and *pgk1Δ* (Figure 3E; quantification in Table S2) cells. Taken together, these results suggest that complete glycolysis with net ATP production is essential for TORC1 activation via the Rag GTPase-independent pathway. Because pyruvate is the end product of glycolysis, we tested whether pyruvate is sufficient for TORC1 activation. Addition of pyruvate to starved yeast cells did not activate TORC1 (Figure S7B; quantification in Table S3). Glycolytic metabolites can serve as precursors for amino acids, which could then activate TORC1. Conversion of the glycolytic metabolite 3-phosphoglycerate to serine and glycine requires the action of the enzymes 3-phosphoglycerate dehydrogenase and 3-phosphoserine aminotransferase by the *SER3* and *SER1* genes, respectively. Pyruvate can generate amino acids glutamate/glutamine from the TCA cycle intermediate α-ketoglutarate via the action of the glutamate dehydrogenases Gdh1 and Gdh2. Glutamine has been shown to activate TORC1 via Pib2 and independent of Rag GTPases.[33,34] We therefore assayed glucose-induced TORC1 activation in wild-type, *ser3Δ*, *ser1Δ*, and *gdh1Δ gdh2Δ* cells and their *gtr1Δ* variants. Glucose activated TORC1 to comparable extents in wild-type, *ser1Δ ser3Δ*, and *gdh1Δ gdh2Δ* cells (with or without Gtr1), suggesting that glutamine/serine production from glycolytic metabolites is not required for the Rag-GTPase-dependent and Rag-GTPase–independent pathways (Figure S7C; quantification in Table S3).

ATP generated by glycolysis could be required for V-ATPase activity. To test whether V-ATPase activity is required for glucose-induced TORC1 activation, we treated nutrient-starved cells with the V-ATPase inhibitor bafilomycin A1,[35] added glucose to wild-type and *gtr1Δ* cells, and assayed TORC1 activation. Bafilomycin A1 treatment had little or no effect of TORC1 activation in wild-type cells (Figure 6C;quantification in

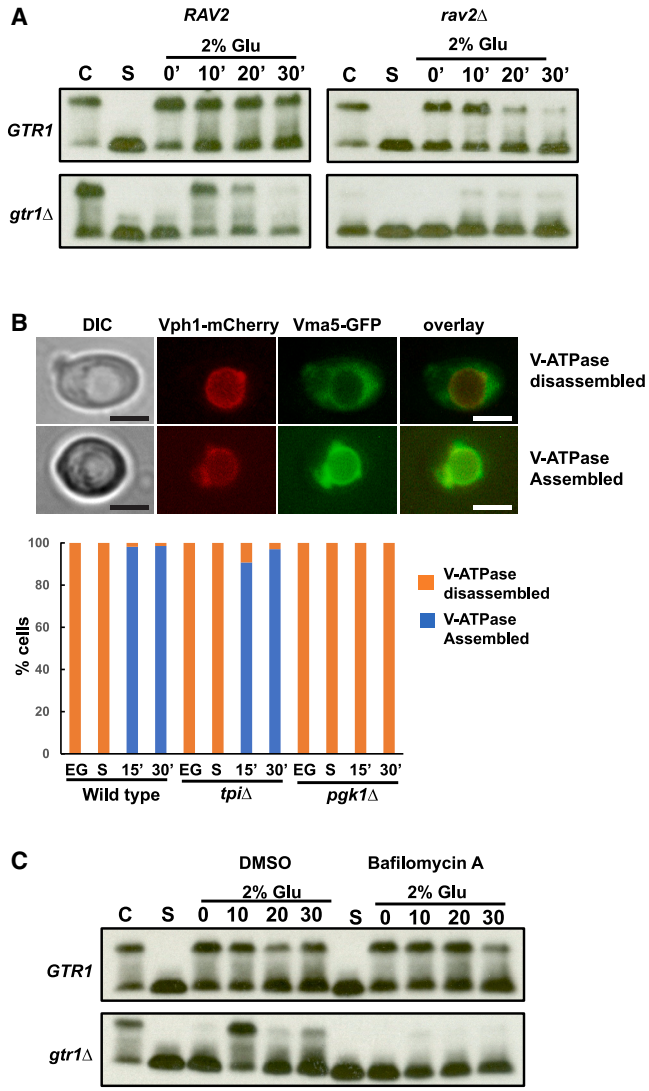

Figure 6. V-ATPase reassembly and activation are required for the Rag GTPase-independent pathway of TORC1 activation

(A) Wild-type, *gtr1Δ*, *rav2Δ*, and *rav2Δ gtr1Δ* cells were grown in logarithmic phase (C) in SC-Glu medium and subjected to complete nutrient starvation by incubating them in water for 1 h. Starved cells (S) were then transferred to a solution containing 2% Glu. Aliquots of the cultures were taken after 0, 10, 20, and 30 min and used for preparing protein extracts. Phosphorylation of Sch9 was monitored by western blotting.

(B) Wild-type, *tpi1Δ* and *pgk1Δ* cells expressing Vma5-GFP and Vph1-mCherry were subjected to the Glu-induced TORC1 activation assay. Aliquots of the cultures were taken at different points and examined by fluorescence microscopy. Percentages of cells showing localization of Vph1-mCherry and Vma5-GFP were plotted. Representative images of cells with assembled and dissembled V-ATPase are shown (N = 500 cells). Scale bars represent 3 μm.

(C) Same as described in (A) but performed with wild-type and *gtr1Δ* cells in the presence and absence of bafilomycin (10 μM).

All data are representative of 3 independent experiments.

Table S2). However, glucose-induced TORC1 activation was severely reduced in bafilomycin A1-treated *gtr1Δ* cells (Figure 6C; quantification in Table S2). Taken together, our results suggest that V-ATPase assembly and activation following glucose addition is required for the Rag GTPase-independent pathway for TORC1 activation.

DISCUSSION

An exciting yet formidable challenge in biology is to understand how a cell senses the presence of nutrients and fine-tunes its growth and developmental state. The discovery and characterization of TORC1 was a significant step toward meeting this challenge in eukaryotic cells. TORC1, a highly conserved eukaryotic protein complex, integrates sensory inputs from growth factors, amino acids, and glucose with rates of cellular growth, metabolism, and proliferation. But the molecular details of how nutrients modulate TORC1 activity remain to be uncovered. Discovery of sestrins provided a mechanistic basis for regulation of mTORC1 activity by amino acids in mammalian cells. However, how amino acids and glucose regulate TORC1 activity in *S. cerevisiae* remains largely unknown. In this study, we combined genetics with targeted metabolite analysis to identify cellular factors and metabolic requirements for glucose-induced TORC1 activation in *S. cerevisiae*. We show that metabolism of glucose via the glycolytic pathway activates TORC1 through three distinct pathways (Figure 7).

A non-canonical pathway for TORC1 activation

Activation of TORC1 via binding of $Gtr1^{GTP}$-$Gtr2^{GDP}$ under conditions of amino acid sufficiency constitutes the canonical pathway of TORC1 activation, which is conserved from yeast to humans. Our work defines a non-canonical pathway of TORC1 activation that is promoted by $Gtr1^{GTP}$-$Gtr2^{GTP}$ but inhibited by $Gtr1^{GTP}$-$Gtr2^{GDP}$. Multiple lines of evidence support the existence of a non-canonical pathway. Either inactivation of SEACIT complexes or expression of $Gtr1^{GTP}$-$Gtr2^{GDP}$ blocked TORC1 activation in 2-DG-treated wild-type cells. Addition of glucose to *pgi1Δ* cells or mannose to *pmi40Δ* cells phenocopied the 2-DG-treated wild-type cells. However, the onset of TORC1 activation in wild-type cells by 2-DG (or in *pmi40Δ* cells by 0.05% mannose) was delayed by about 10 min compared to the onset of glucose-induced TORC1 activation in *pgi1Δ* cells. This delay could be due to hexokinases having a reduced substrate preference for 2-DG and mannose in comparison with glucose. Alternatively, the delay could be due to 2-DG's reported effects on N-glycosylation of proteins[36] and endoplasmic reticulum (ER) stress-induced autophagy[37] by mimicking mannose 6-phosphate.

The non-canonical pathway was active in 2-DG-treated cells expressing either wild-type Gtr1/Gtr2 or $Gtr1^{GTP}$-$Gtr2^{GTP}$. SEACIT mutant cells accumulated $Gtr1^{GTP}$ but failed to activate the non-canonical pathway. We reasoned that hydrolysis of GTP bound to Gtr1 might help GTP binding/GDP dissociation from Gtr2, thereby preventing the formation of $Gtr1^{GTP}$-$Gtr2^{GTP}$ in SEACIT mutant cells. Consistent with this possibility, the failure of SEACIT mutant cells to activate the non-canonical pathway was suppressed by expression of the $Gtr2^{GTP}$ bound form. Because SEACIT mutant cells accumulate $Gtr1^{GTP}$ bound form, this further shows that $Gtr1^{GTP}$-$Gtr2^{GTP}$ promotes the non-canonical pathway of TORC1 activation.

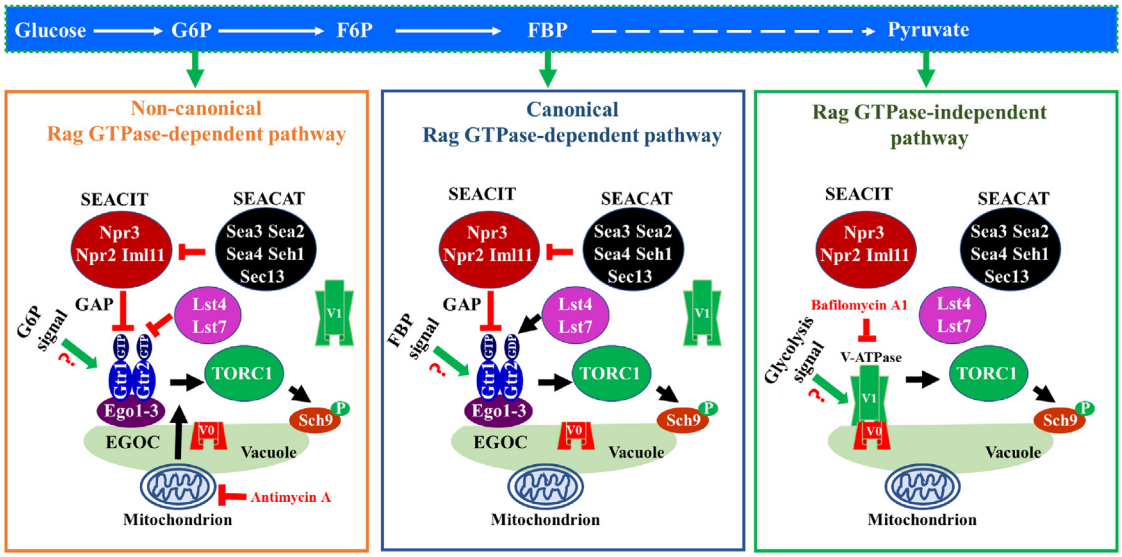

Figure 7. A model for Glu-induced TORC1 activation
Please see the text for details.

Intriguingly, mitochondrial function is required for the non-canonical pathway of TORC1 activation. Petite mutation or addition of antimycin compromised 2-DG-induced TORC1 activation. Precisely how mitochondrial function promotes the non-canonical pathway is not addressed in this study. Mitochondria could provide ATP for sustaining the non-canonical pathway. Physical connections between mitochondria and vacuole have been reported to be mediated by Vps39/Vam6 and Vps13 in yeast.[38] Interestingly, Vps39/Vam6 has also been shown to regulate TORC1 activity via Rag1 GTPase.[6] It is also noteworthy that antimycin treatment had a modest effect on the Rag GTPase-independent pathway, which requires V-ATPase function.

What might be the function of non-canonical pathway? One possibility is that yeast cells might use two different pathways to activate TORC1 during glycolysis and gluconeogenesis. During glycolysis, FBP activates TORC1 via the canonical pathway. During gluconeogenesis, G6P might activate TORC1 via the non-canonical pathway. Interestingly, mitochondrial function essential for energy generation during gluconeogenesis is required for the non-canonical pathway. Having two separate mechanisms for TORC1 activation could facilitate specificity of downstream responses during glycolysis and gluconeogenesis. Uncovering the biological relevance of the non-canonical pathway of TORC1 activation and whether this pathway is conserved in mammalian cells is an exciting challenge for the future. Intriguingly, G6P activates mTORC1 in mammalian cells.[39] As observed in yeast, mTORC1 was activated by lower concentrations of 2-DG but inhibited at higher concentrations.[39] Upon G6P deprivation, hexokinase II bound and inhibited TORC1 through its TOS (TOR signaling) motif. In the presence of glucose, G6P is formed, which binds to hexokinase II (HK-II) and releases it from TORC1, thus relieving the inhibition. Testing whether 2-DG activation in mammalian cells is dependent on canonical/non-canonical states of the RagA/B-RagC/D heterodimer would be informative.

How might the non-canonical pathway work? One possibility is that the TORC1 in starved cells adopts a different higher-order structure that requires $Gtr1^{GTP}$-$Gtr2^{GTP}$ instead of $Gtr1^{GTP}$-$Gtr2^{GDP}$ for activation. G6P could either directly or indirectly alter the TORC1 complex structure to facilitate interaction with the $Gtr1^{GTP}$-$Gtr2^{GTP}$. TORC1 forms TOROIDs during starvation in yeast, which requires the inactive heterodimer $Gtr1^{GDP}$-$Gtr2^{GTP}$. However, we did not observe any TORC1 foci during complete nutrient starvation (M.A. and P.A., unpublished data). Also, expression of $Gtr1^{GDP}$-$Gtr2^{GTP}$ did not activate the non-canonical pathway (Figure 2B; quantification in Table S2).

Canonical pathway of glucose-induced TORC1 activation

Activation of canonical pathway requires active $Gtr1^{GTP}$-$Gtr2^{GDP}$ and formation of FBP. Inactivation of the SEACIT complex or expression of $Gtr1^{GTP}$-$Gtr2^{GDP}$ boosted the canonical pathway indicated by steady levels of Sch9 phosphorylation in the SEACIT mutants. Presumably, the phosphorylation status of Sch9 is determined by outcome of a tug of-war between kinases (TORC1) and phosphatases. Because inactivation of SEACIT is expected to reduce downregulation of TORC1 activity by locking Gtr1 in the GTP-bound state, TORC1 activity is stabilized, resulting in steady levels of Sch9 phosphorylation.

While blocking glycolysis before FBP formation prevented activation of the canonical pathway, blocking glycolysis downstream of FBP formation did not affect this pathway. Inactivation of aldolase, which boosted FBP levels, hyperactivated TORC1, although transiently. How might FBP activate TORC1? FBP has been shown to inactivate AMPK in human cells by binding to aldolase.[26] It is very unlikely that FBP binds to aldolase in yeast to activate TORC1 via a non-enzymatic function. Although yeast aldolase and human aldolase A catalyze the same enzymatic reaction, they are not homologs and evolved convergently to perform the same function. Human aldolase was able to

substitute for yeast aldolase functionally in glycolysis and TORC1 activation. FBP also binds with other two proteins, Fbp1 and Cdc19, which have FBPase and pyruvate kinase activity, respectively. Deletion of *FBP1*, which encodes FBPase, did not affect TORC1 activation. FBP binds to Cdc19 and activates its enzymatic activity allosterically. However, a constitutively active form of Cdc19 that lacks FBP binding was comparable with wild-type Cdc19 in terms of activating the canonical pathway of glucose-induced TORC1 activation. *pgk1Δ* cells accumulated FBP during starvation but failed to activate TORC1. We hypothesize that the production of FBP from glucose but not FBP itself is required for TORC1 activation. The old adage "the journey is more important than the destination" might be an appropriate description of the effect of glycolysis on the canonical pathway of TORC1 activation.

Our results suggest that signals generated by metabolism of glucose to FBP activates TORC1 independent of the SEACIT complex. In starved SEACIT mutant cells, TORC1 is inactive, and addition of glucose activates TORC1 (Figure 2A). This indicates that glucose-induced TORC1 activation is not mediated via inhibition of SEACIT complex. We suggest that a signal caused by FBP formation promotes TORC1 activity by generating the $Gtr1^{GTP}$-$Gtr2^{GDP}$-bound form. This could occur via activation of factors that facilitate exchange of GDP by GTP in Gtr1. Determining how FBP formation activates TORC1 is an important challenge for the future.

Interestingly, DHAP has been shown to be required for glucose-dependent mTORC1 activation in human cells.[40] Moreover, conversion of Dihydroxyacetone (DHA) to DHAP by triose kinase was sufficient to activate mTORC1 in the absence of glucose.[40] It is possible that eukaryotic cells might have evolved different mechanism to link the presence of glucose with TORC1 activation.

TORC1 is activated via the Rag GTPase-independent pathway

Our results support the notion that complete glycolysis is required for glucose-induced activation of TORC1 via the Rag GTPase-independent pathway. Blocking glycolysis via deleting/transcriptionally silencing genes that encode aldolase, triose-phosphate isomerase, phosphoglyceraldehyde dehydrogenase, and phosphoglycerate kinase did not affect the Rag GTPase-dependent canonical pathway but abolished the Rag GTPase-independent pathway. Phenotypes of the *rav2Δ* cells and bafilomycin-treated *gtr1Δ* cells suggest that V-ATPase reassembly and V-ATPase activity are required for TORC1 activation via the Rag GTPase-independent pathway.

Disassembly of V-ATPase during glucose starvation in yeast is a well-known phenomenon.[30] The V-ATPase consists of the membrane-bound Vo sector that forms the proton pore and the cytosolic V1 sector, which has ATPase activity. V-ATPase catalyzes ATP-dependent uptake of protons into the vacuole to regulates cytosolic pH. Glucose starvation results in dissociation of V1 from Vo and consequent inhibition of V-ATPase activity. Re-addition of glucose drives the reassembly of V-ATPase, which is facilitated by the RAVE complex. We propose that V-ATPase reassembly and activation following glucose metabolism acidifies the vacuole, which activates TORC1 resident in the vacuole. TORC1 activation in *gtr1Δ* cells is slower by about 10 min relative to wild-type cells. Complete glycolysis and vacuolar acidification might take additional time, which could account for the delay. The *tpi1Δ* mutant helped to uncouple V-ATPase assembly from glucose-induced TORC1 activation. Both V-ATPase assembly and ATP generation induced by glycolysis are required for TORC1 activation. Production of ATP via glycolysis could promote V-ATPase activity. Alternatively, metabolites derived from complete glycolysis could facilitate V-ATPase activation. Pyruvate addition to starved cells was insufficient to activate TORC1 (Figure S7B; quantification in Table S3). A previous study proposed that glucose regulates TORC1 by regulating the cytosolic pH via Gtr1.[20] However, our results indicate that V-ATPase regulates TORC1 independent of Gtr1. Treatment with bafilomycin had very little effect on TORC1 activation via the canonical and non-canonical pathways dependent on Rag GTPases.

Relative contribution of the three pathways to glucose-induced TORC1 activation

Comparison of TORC1 activation in wild-type and *gtr1Δ* strains suggests that the Rag GTPase-dependent pathway contributes to the bulk of TORC1 activity in the first 10 min. Antimycin A treatment blocks the non-canonical pathway (2-DG-treated wild-type cells or 2% glucose-treated *pgi1Δ* cells) but had no effect on TORC1 activation in 2% glucose-treated wild-type cells. This suggests that either the canonical/non-canonical pathways do not operate simultaneously or that the non-canonical pathway's contribution to TORC1 activation in 2% glucose-treated wild-type cells is minor. Likewise, bafilomycin treatment had little effect on TORC1 activation in glucose-treated wild-type cells but severely affected TORC1 activation in *gtr1Δ* cells. This suggests that the Rag-GTPase-independent pathway makes a minor contribution to the TORC1 activation in wild-type cells. However, it is unknown whether all three pathways can operate simultaneously and independently *in vivo* and whether they are influenced by mutual synergy/antagonism. For both Rag GTPase-dependent pathways to be active, the $Gtr1^{GTP}$-$Gtr2^{GDP}$ and $Gtr1^{GTP}$-$Gtr2^{GTP}$ complexes should co-exist. Determining the relative contribution of the 3 pathways for TORC1 activation and their underlying molecular mechanisms and physiological relevance is of pivotal importance.

In complete contrast to TORC1, the energy-sensing kinase Snf1/AMPK is active in glucose-starved yeast cells and inactive in glucose-treated cells.[41] AMPK has been shown to inhibit TORC1 in yeast by phosphorylating Kog1.[18] More recently, Snf1/AMPK has been shown to inhibit TORC1 during glucose starvation via Pib2 and by phosphorylating the N-terminal domain of Sch9.[42] A reciprocal antagonistic regulation of TORC1 and AMPK activities has been observed in fission yeast and mammalian cells.[43] It might be informative to test the role of Snf1 and its phospho-substrates in the three pathways of glucose-induced TORC1 activation.

In summary, we have identified three different pathways through which glucose activates TORC1 (Figure 7). We show that G6P, FBP, and complete glycolysis are required for the non-canonical (Rag GTPase-dependent), canonical (Rag GTPase-dependent), and Rag GTPase-independent pathways,

respectively. While our *in vivo* assay has certain limitations, our work sets a foundation to dissect the mechanism of glucose-induced TORC1 activation. An *in vitro*/extract-based assay will help to confirm and dissect the specific molecular activators of TORC1.

Glucose uptake and metabolism are often elevated in cancer cells.[44] Cancer cells aerobically metabolize glucose and produce lactate even in the presence of mitochondria. This phenomenon of aerobic glycolysis is known as the "Warburg effect." However, how the Warburg effect benefits the growth and survival of cancer cells is not resolved. While our study shows that glycolytic metabolites activate TORC1 by multiple mechanisms in yeast, DHAP has been shown to be sufficient to activate mTORC1 in human cells.[40] It is possible that cancer cells might use glycolysis to boost mTORC1 activity and positively regulate growth and proliferation. Interestingly, mTORC1 activity is found to be upregulated in several forms of cancer.[5] Uncovering the link between glycolysis and mTORC1 activity could identify novel targets for cancer therapy.

Limitations of the study

We defined the relationship between TORC1 and glucose metabolism by performing a glucose-induced TORC1 activation assay in mutants defective in various steps of glycolysis. It is possible that the glycolytic mutations have pleiotropic effects on cell physiology, which could directly or indirectly affect TORC1 function. Indeed, TORC1 activation was inhibited at high glucose concentrations in a few glycolytic mutants. An *in vitro* assay for glucose-induced TORC1 activation using purified protein complexes will help to test several predictions from our study. Quantification of TORC1 activation data in our study was based on one representative replicate. Inclusion of additional replicates for quantification may better support some conclusions. A real-time *in vivo* assay for glucose-induced TORC1 activation will facilitate a quantitative analysis of the relative contributions of the three pathways. Finally, we did not identify residues in Sch9 that are phosphorylated by TORC1. Phosphoproteomics analyses may help to identify pathway-specific phosphorylation events in Sch9 and other TORC1 substrates.

STAR★METHODS

Detailed methods are provided in the online version of this paper and include the following:

- KEY RESOURCES TABLE
- RESOURCE AVAILABILITY
  - Lead contact
  - Materials availability
  - Data and code availability
- EXPERIMENTAL MODEL AND STUDY PARTICIPANT DETAILS
  - Yeast strains and oligos
  - Chemical treatment to cell culture
- METHOD DETAILS
  - TORC1 activity assay
  - Quantification of western blot images
  - Analysis of glycolytic metabolites
  - ATP analysis
  - Microscopy
- QUANTIFICATION AND STATISTICAL ANALYSIS

SUPPLEMENTAL INFORMATION

Supplemental information can be found online at https://doi.org/10.1016/j.celrep.2023.113205.

ACKNOWLEDGMENTS

We thank Prof. Claudio de Virgilio (University of Fribourg, Switzerland), Prof. Mike Hall (Biozentrum University of Basel, Switzerland), Prof. Capaldi (University of Arizona, USA), and Prof. Sheng-Cai Lin (Xiamen University, China) for sharing plasmids and strains. We would like to acknowledge A*STAR (Singapore)'s core funding provided to the Arumugam laboratory and A*STAR (Singapore)'s Career Development Fund (C210112008) to the Alfatah laboratory.

AUTHOR CONTRIBUTIONS

M.A. designed and performed TORC1 activation assay experiments, metabolite preparations, and V-ATPase reassembly experiments; supervised T.Y.N.C., Y.Z., and A.N.; and contributed to writing the manuscript. L.C. performed and analyzed the mass spectrometry experiments. C.J.H.G., T.Y.N.C., Y.Z., A.N., J.H.W., and W.J.P. performed TORC1 activation assays. T.Y.N.C. and Y.Z. performed ATP analysis. J.L. performed the V-ATPase reassembly experiments. P.A. conceived and supervised the project and wrote the manuscript. All authors have read the manuscript.

DECLARATION OF INTERESTS

The authors declare no competing interests.

Received: April 20, 2022
Revised: July 30, 2023
Accepted: September 18, 2023
Published: October 4, 2023

REFERENCES

1. González, A., and Hall, M.N. (2017). Nutrient sensing and TOR signaling in yeast and mammals. EMBO J. *36*, 397–408. https://doi.org/10.15252/embj.201696010.
2. Powis, K., and De Virgilio, C. (2016). Conserved regulators of Rag GTPases orchestrate amino acid-dependent TORC1 signaling. Cell Discov. *2*, 15049. https://doi.org/10.1038/celldisc.2015.49.
3. Binda, M., Bonfils, G., Panchaud, N., Péli-Gulli, M.P., and De Virgilio, C. (2010). An EGOcentric view of TORC1 signaling. Cell Cycle *9*, 221–222. https://doi.org/10.4161/cc.9.2.10585.
4. Panchaud, N., Péli-Gulli, M.P., and De Virgilio, C. (2013). SEACing the GAP that nEGOCiates TORC1 activation: evolutionary conservation of Rag GTPase regulation. Cell Cycle *12*, 2948–2952. https://doi.org/10.4161/cc.26000.
5. Saxton, R.A., and Sabatini, D.M. (2017). mTOR Signaling in Growth, Metabolism, and Disease. Cell *168*, 960–976. https://doi.org/10.1016/j.cell.2017.02.004.
6. Binda, M., Péli-Gulli, M.P., Bonfils, G., Panchaud, N., Urban, J., Sturgill, T.W., Loewith, R., and De Virgilio, C. (2009). The Vam6 GEF controls TORC1 by activating the EGO complex. Mol. Cell *35*, 563–573. https://doi.org/10.1016/j.molcel.2009.06.033.
7. Hatakeyama, R., Péli-Gulli, M.P., Hu, Z., Jaquenoud, M., Garcia Osuna, G.M., Sardu, A., Dengjel, J., and De Virgilio, C. (2019). Spatially Distinct Pools of TORC1 Balance Protein Homeostasis. Mol. Cell *73*, 325–338.e8. https://doi.org/10.1016/j.molcel.2018.10.040.

8. Sancak, Y., Bar-Peled, L., Zoncu, R., Markhard, A.L., Nada, S., and Sabatini, D.M. (2010). Ragulator-Rag complex targets mTORC1 to the lysosomal surface and is necessary for its activation by amino acids. Cell *141*, 290–303. https://doi.org/10.1016/j.cell.2010.02.024.

9. Nicastro, R., Sardu, A., Panchaud, N., and De Virgilio, C. (2017). The Architecture of the Rag GTPase Signaling Network. Biomolecules *7*, 48. https://doi.org/10.3390/biom7030048.

10. Chantranupong, L., Wolfson, R.L., Orozco, J.M., Saxton, R.A., Scaria, S.M., Bar-Peled, L., Spooner, E., Isasa, M., Gygi, S.P., and Sabatini, D.M. (2014). The Sestrins interact with GATOR2 to negatively regulate the amino-acid-sensing pathway upstream of mTORC1. Cell Rep. *9*, 1–8. https://doi.org/10.1016/j.celrep.2014.09.014.

11. Saxton, R.A., Knockenhauer, K.E., Schwartz, T.U., and Sabatini, D.M. (2016). The apo-structure of the leucine sensor Sestrin2 is still elusive. Sci. Signal. *9*, ra92. https://doi.org/10.1126/scisignal.aah4497.

12. Saxton, R.A., Knockenhauer, K.E., Wolfson, R.L., Chantranupong, L., Pacold, M.E., Wang, T., Schwartz, T.U., and Sabatini, D.M. (2016). Structural basis for leucine sensing by the Sestrin2-mTORC1 pathway. Science *351*, 53–58. https://doi.org/10.1126/science.aad2087.

13. Wolfson, R.L., Chantranupong, L., Saxton, R.A., Shen, K., Scaria, S.M., Cantor, J.R., and Sabatini, D.M. (2016). Sestrin2 is a leucine sensor for the mTORC1 pathway. Science *351*, 43–48. https://doi.org/10.1126/science.aab2674.

14. Bonfils, G., Jaquenoud, M., Bontron, S., Ostrowicz, C., Ungermann, C., and De Virgilio, C. (2012). Leucyl-tRNA synthetase controls TORC1 via the EGO complex. Mol. Cell *46*, 105–110. https://doi.org/10.1016/j.molcel.2012.02.009.

15. Urban, J., Soulard, A., Huber, A., Lippman, S., Mukhopadhyay, D., Deloche, O., Wanke, V., Anrather, D., Ammerer, G., Riezman, H., et al. (2007). Sch9 is a major target of TORC1 in Saccharomyces cerevisiae. Mol. Cell *26*, 663–674. https://doi.org/10.1016/j.molcel.2007.04.020.

16. Alfatah, M., Wong, J.H., Krishnan, V.G., Lee, Y.C., Sin, Q.F., Goh, C.J.H., Kong, K.W., Lee, W.T., Lewis, J., Hoon, S., and Arumugam, P. (2021). TORC1 regulates the transcriptional response to glucose and developmental cycle via the Tap42-Sit4-Rrd1/2 pathway in Saccharomyces cerevisiae. BMC Biol. *19*, 95. https://doi.org/10.1186/s12915-021-01030-3.

17. Hughes Hallett, J.E., Luo, X., and Capaldi, A.P. (2014). State transitions in the TORC1 signaling pathway and information processing in Saccharomyces cerevisiae. Genetics *198*, 773–786. https://doi.org/10.1534/genetics.114.168369.

18. Hughes Hallett, J.E., Luo, X., and Capaldi, A.P. (2015). Snf1/AMPK promotes the formation of Kog1/Raptor-bodies to increase the activation threshold of TORC1 in budding yeast. Elife *4*, e09181. https://doi.org/10.7554/eLife.09181.

19. Kane, P.M., and Smardon, A.M. (2003). Assembly and regulation of the yeast vacuolar H+-ATPase. J. Bioenerg. Biomembr. *35*, 313–321. https://doi.org/10.1023/a:1025724814656.

20. Dechant, R., Saad, S., Ibáñez, A.J., and Peter, M. (2014). Cytosolic pH regulates cell growth through distinct GTPases, Arf1 and Gtr1, to promote Ras/PKA and TORC1 activity. Mol. Cell *55*, 409–421. https://doi.org/10.1016/j.molcel.2014.06.002.

21. Prouteau, M., Desfosses, A., Sieben, C., Bourgoint, C., Lydia Mozaffari, N., Demurtas, D., Mitra, A.K., Guichard, P., Manley, S., and Loewith, R. (2017). TORC1 organized in inhibited domains (TOROIDs) regulate TORC1 activity. Nature *550*, 265–269. https://doi.org/10.1038/nature24021.

22. Xu, Y.F., Zhao, X., Glass, D.S., Absalan, F., Perlman, D.H., Broach, J.R., and Rabinowitz, J.D. (2012). Regulation of yeast pyruvate kinase by ultrasensitive allostery independent of phosphorylation. Mol. Cell *48*, 52–62. https://doi.org/10.1016/j.molcel.2012.07.013.

23. Kondo, T., and Beutler, E. (1979). Depletion of red cell ATP by incubation with 2-deoxyglucose. J. Lab. Clin. Med. *94*, 617–623.

24. Péli-Gulli, M.P., Sardu, A., Panchaud, N., Raucci, S., and De Virgilio, C. (2015). Amino Acids Stimulate TORC1 through Lst4-Lst7, a GTPase-Activating Protein Complex for the Rag Family GTPase Gtr2. Cell Rep. *13*, 1–7. https://doi.org/10.1016/j.celrep.2015.08.059.

25. Slater, E.C. (1973). The mechanism of action of the respiratory inhibitor, antimycin. Biochim. Biophys. Acta *301*, 129–154. https://doi.org/10.1016/0304-4173(73)90002-5.

26. Zhang, C.S., Hawley, S.A., Zong, Y., Li, M., Wang, Z., Gray, A., Ma, T., Cui, J., Feng, J.W., Zhu, M., et al. (2017). Fructose-1,6-bisphosphate and aldolase mediate glucose sensing by AMPK. Nature *548*, 112–116. https://doi.org/10.1038/nature23275.

27. Marsh, J.J., and Lebherz, H.G. (1992). Fructose-bisphosphate aldolases: an evolutionary history. Trends Biochem. Sci. *17*, 110–113. https://doi.org/10.1016/0968-0004(92)90247-7.

28. Jurica, M.S., Mesecar, A., Heath, P.J., Shi, W., Nowak, T., and Stoddard, B.L. (1998). The allosteric regulation of pyruvate kinase by fructose-1,6-bisphosphate. Structure *6*, 195–210. https://doi.org/10.1016/s0969-2126(98)00021-5.

29. Fenton, A.W., and Blair, J.B. (2002). Kinetic and allosteric consequences of mutations in the subunit and domain interfaces and the allosteric site of yeast pyruvate kinase. Arch. Biochem. Biophys. *397*, 28–39. https://doi.org/10.1006/abbi.2001.2634.

30. Hayek, S.R., Rane, H.S., and Parra, K.J. (2019). Reciprocal Regulation of V-ATPase and Glycolytic Pathway Elements in Health and Disease. Front. Physiol. *10*, 127. https://doi.org/10.3389/fphys.2019.00127.

31. Smardon, A.M., Diab, H.I., Tarsio, M., Diakov, T.T., Nasab, N.D., West, R.W., and Kane, P.M. (2014). The RAVE complex is an isoform-specific V-ATPase assembly factor in yeast. Mol. Biol. Cell *25*, 356–367. https://doi.org/10.1091/mbc.E13-05-0231.

32. Smardon, A.M., Tarsio, M., and Kane, P.M. (2002). The RAVE complex is essential for stable assembly of the yeast V-ATPase. J. Biol. Chem. *277*, 13831–13839. https://doi.org/10.1074/jbc.M200682200.

33. Tanigawa, M., Yamamoto, K., Nagatoishi, S., Nagata, K., Noshiro, D., Noda, N.N., Tsumoto, K., and Maeda, T. (2021). A glutamine sensor that directly activates TORC1. Commun. Biol. *4*, 1093. https://doi.org/10.1038/s42003-021-02625-w.

34. Tanigawa, M., and Maeda, T. (2017). An In Vitro TORC1 Kinase Assay That Recapitulates the Gtr-Independent Glutamine-Responsive TORC1 Activation Mechanism on Yeast Vacuoles. Mol. Cell Biol. *37*, e00075-17. https://doi.org/10.1128/MCB.00075-17.

35. Bowman, E.J., Siebers, A., and Altendorf, K. (1988). Bafilomycins: a class of inhibitors of membrane ATPases from microorganisms, animal cells, and plant cells. Proc. Natl. Acad. Sci. USA *85*, 7972–7976. https://doi.org/10.1073/pnas.85.21.7972.

36. Laussel, C., and Léon, S. (2020). Cellular toxicity of the metabolic inhibitor 2-deoxyglucose and associated resistance mechanisms. Biochem. Pharmacol. *182*, 114213. https://doi.org/10.1016/j.bcp.2020.114213.

37. Xi, H., Kurtoglu, M., Liu, H., Wangpaichitr, M., You, M., Liu, X., Savaraj, N., and Lampidis, T.J. (2011). 2-Deoxy-D-glucose activates autophagy via endoplasmic reticulum stress rather than ATP depletion. Cancer Chemother. Pharmacol. *67*, 899–910. https://doi.org/10.1007/s00280-010-1391-0.

38. Elbaz-Alon, Y., Rosenfeld-Gur, E., Shinder, V., Futerman, A.H., Geiger, T., and Schuldiner, M. (2014). A dynamic interface between vacuoles and mitochondria in yeast. Dev. Cell *30*, 95–102. https://doi.org/10.1016/j.devcel.2014.06.007.

39. Roberts, D.J., Tan-Sah, V.P., Ding, E.Y., Smith, J.M., and Miyamoto, S. (2014). Hexokinase-II positively regulates glucose starvation-induced autophagy through TORC1 inhibition. Mol. Cell *53*, 521–533. https://doi.org/10.1016/j.molcel.2013.12.019.

40. Orozco, J.M., Krawczyk, P.A., Scaria, S.M., Cangelosi, A.L., Chan, S.H., Kunchok, T., Lewis, C.A., and Sabatini, D.M. (2020). Dihydroxyacetone

phosphate signals glucose availability to mTORC1. Nat. Metab. *2*, 893–901. https://doi.org/10.1038/s42255-020-0250-5.

41. Wilson, W.A., Hawley, S.A., and Hardie, D.G. (1996). Glucose repression/derepression in budding yeast: SNF1 protein kinase is activated by phosphorylation under derepressing conditions, and this correlates with a high AMP:ATP ratio. Curr. Biol. *6*, 1426–1434. https://doi.org/10.1016/s0960-9822(96)00747-6.

42. Caligaris, M., Nicastro, R., Hu, Z., Tripodi, F., Hummel, J.E., Pillet, B., Deprez, M.A., Winderickx, J., Rospert, S., Coccetti, P., et al. (2023). Snf1/AMPK fine-tunes TORC1 signaling in response to glucose starvation. Elife *12*. https://doi.org/10.7554/eLife.84319.

43. Ling, N.X.Y., Kaczmarek, A., Hoque, A., Davie, E., Ngoei, K.R.W., Morrison, K.R., Smiles, W.J., Forte, G.M., Wang, T., Lie, S., et al. (2020). mTORC1 directly inhibits AMPK to promote cell proliferation under nutrient stress. Nat. Metab. *2*, 41–49. https://doi.org/10.1038/s42255-019-0157-1.

44. Hay, N. (2016). Reprogramming glucose metabolism in cancer: can it be exploited for cancer therapy? Nat. Rev. Cancer *16*, 635–649. https://doi.org/10.1038/nrc.2016.77.

45. Zhong, W., Cui, L., Goh, B.C., Cai, Q., Ho, P., Chionh, Y.H., Yuan, M., Sahili, A.E., Fothergill-Gilmore, L.A., Walkinshaw, M.D., et al. (2017). Allosteric pyruvate kinase-based "logic gate" synergistically senses energy and sugar levels in Mycobacterium tuberculosis. Nat. Commun. *8*, 1986. https://doi.org/10.1038/s41467-017-02086-y.

STAR★METHODS

KEY RESOURCES TABLE

REAGENT or RESOURCE	SOURCE	IDENTIFIER
Antibodies		
Anti-HA High Affinity; Rat monoclonal antibody (clone 3F10)	Roche Cat# 11867423001	RRID:AB_390918
Goat anti-rat IgG-HRP	Santa Cruz Biotechnology Cat# sc-2032	RRID:AB_631755
Chemicals, peptides, and recombinant proteins		
Dimethyl sulfoxide	MP Biomedicals	Cat#196055; CAS: 67-68-5
Rapamycin	Enzo	Cat#BML-A275-0025
Antimycin A	Sigma	Cat#A8674; CAS: 1397-94-0
Bafilomycin A1	Cayman Chemical	Cat# 11038; CAS: 88899-55-2
Trichloroacetic Acid	Sigma	Cat#T6399; CAS: 7603-9
2-(Cyclohexylamino)ethanesulfonic acid (CHES)	Sigma	Cat#C2885; CAS: 103-47-9
Tris(2-carboxyethyl)phosphine hydrochloride (TCEP)	Sigma	Cat#68957; CAS: 51805-45-9
2-Nitro-5-thiocyanatobenzoic Acid (NTCB)	Tokyo Chemical Industry Co. Ltd.	Cat#N0516; CAS: 30211-77-9
Phenylmethanesulfonyl Fluoride (PMSF)	Sigma	Cat#36978; CAS: 329-98-6
PhosSTOP	Roche	Cat#04906837001
EDTA	Promega	Cat#V4233
10% Sodium Dodecyl Sulfate	1st Base	Cat#BUF-2051-500mL
10X Tris-Glycine Sodium Dodecyl Sulfate	1st Base	Cat#BUF-2030-10X4L
10X Phosphate Buffered Saline	1st Base	Cat#BUF-2040-1X1L
Yeast extract	BD Biosciences	Cat#212750
Peptone	BD Biosciences	Cat#211677
Agar	BD Diagnostics	Cat#214010
Dextrose	Bio Basic	Cat#GB0219; CAS: 50-99-7
Glycerol	Sigma	Cat#G9012; CAS: 56-81-5
Yeast nitrogen base without amino acids	BD Biosciences	Cat#291940
Critical commercial assays		
PhosphoWorks™ Luminometric ATP Assay Kit	AAT Bioquest	Cat#21610
Protein Assay Dye Reagent Concentrate	Bio-Rad	Cat#500-0006
YeaStar Genomic DNA Kit™	Zymo Research	Cat#D2002
Experimental models: Organisms/strains		
Strain 3526 *(MATa sch9: SCH9-HA6::KanMX6)*	Alfatah et al.[16]	Figures 1–4, 6, S1 and S4–S7
Strain 3869 (*MATa sch9: SCH9-HA6::KanMX6 hxk1::NatMX6 hxk2:HphMX6 glk1::NatMX6)*	This paper	Figure 1
Strain 3681(*MATa gtr1::KanMX6 sch9: SCH9-HA6::KANMX6)*	Alfatah et al.[16]	Figures 1, 2, 3, 4, 6, S4, S5 and S7
Strain 3920 (*MATa sch9: SCH9-HA6::KanMX6 zwf1::NatMX6)*	This paper	Figure S2
Strain 3949 (*MATa sch9: SCH9-HA6::KanMX6 zwf1::NatMX6 gtr1::KanMX6)*	This paper	Figure S2

(*Continued on next page*)

Continued

REAGENT or RESOURCE	SOURCE	IDENTIFIER
Strain 3916 *(MATa sch9: SCH9-HA6::KanMX6 pfk1::NatMX6)*	This paper	Figure S2
Strain 3947 *(MATa sch9: SCH9-HA6::KanMX6 pfk1::NatMX6 gtr1::KanMX6)*	This paper	Figure S2
Strain 3833 (*MATa sch9: SCH9-HA6::KanMX6 iml1::KanMX6)*	This paper	Figures 2 and S3
Strain 4018 *(MATa sch9: SCH9-HA6::KanMX6 iml1::KanMX6 gtr1::KanMX6)*	This paper	Figures 2 and S3
Strain 3831(*MATa sch9: SCH9-HA6::KanMX6 npr2::HIS3MX6)*	This paper	Figures 2 and S3
Strain 4016 (*MATa sch9: SCH9-HA6::KanMX6 npr2::HIS3MX6 gtr1::KanMX6)*	This paper	Figures 2 and S3
Strain 3829 (*MATa sch9: SCH9-HA6::KanMX6 npr3::His3MX6)*	This paper	Figures 2 and S3
Strain 4014 (*MATa sch9: SCH9-HA6::KanMX6 npr3::HIS3MX6 gtr1::KanMX6)*	This paper	Figures 2 and S3
Strain 4050 (*MATa sch9: SCH9-HA6::KanMX6 gtr1::KanMX6 gtr2::KanMX6 TetO7-GTR1 -YCplac33-URA3 TetO7-GTR2 -YCplac111-LEU2)*	This paper	Figures 2 and 4
Strain 4051(*MATa sch9: SCH9-HA6::KanMX6 gtr1::KanMX6 gtr2::KanMX6 TetO7-gtr1-Q65L -YCplac33-URA3 TetO7-gtr2-S23L -YCplac111-LEU2)*	This paper	Figure 2
Strain 4052 *(MATa sch9: SCH9-HA6::KanMX6 gtr1::KanMX6 gtr2::KanMX6 TetO7-gtr1-S20L -YCplac33-URA3 TetO7-gtr2-Q66L -YCplac111-LEU2)*	This paper	Figure 2
Strain 4053 (*MATa sch9: SCH9-HA6::KanMX6 gtr1::KanMX6 gtr2::KanMX6 YCplac33-URA3 YCplac111-LEU2)*	This paper	Figure 2
Strain 3925 (*MATa sch9: SCH9-HA6::KanMX6 pgi1::NatMX6)*	This paper	Figures 2 and S4
Strain 3963 (*MATa sch9: SCH9-HA6::KanMX6 pgi1::NatMX6 gtr1::KanMX6)*	This paper	Figures 2 and S4
Strain 4078 (*MATa sch9: SCH9-HA6::KanMX6 pgi1::NatMX6 npr3::NatMX6)*	This paper	Figure 2
Strain 5031(*MATa sch9: SCH9-HA6::KanMX6 pmi40::HphMX6)*	This paper	Figure S4
Strain 5033(*MATa sch9: SCH9-HA6::KanMX6 pmi40::HphMX6 gtr1::KanMX6)*	This paper	Figure S4
Strain 4099 *(MATa sch9: SCH9-HA6::KanMX6 gtr1::KanMX6 gtr2::KanMX6 TetO7-gtr1-S20L -YCplac33-URA3 TetO7-gtr2-S23L -YCplac111-LEU2)*	This paper	Figure 2

(*Continued on next page*)

Continued

REAGENT or RESOURCE	SOURCE	IDENTIFIER
Strain 4097 (*MATa sch9: SCH9-HA6::KanMX6 gtr1::KanMX6 gtr2::KanMX6 TetO7-gtr1-Q65L -YCplac33-URA3 TetO7-gtr2-Q66L -YCplac111-LEU2)*	This paper	Figures 2 and 4
Strain 4923 (*MATa sch9: SCH9-HA6::KanMX6 gtr1::KanMX6 gtr2::KanMX6 npr3:His3MX6 TetO7-GTR1 -YCplac33-URA3 TetO7-GTR2 -YCplac111-LEU2)*	This paper	Figure 2
Strain 4924 (*MATa sch9: SCH9-HA6::KanMX6 gtr1::KanMX6 gtr2::KanMX6 npr3:His3MX6 TetO7-gtr1-Q65L-YCplac33-URA3 TetO7-gtr2-S23L -YCplac111-LEU2)*	This paper	Figure 2
Strain 4925 (*MATa sch9: SCH9-HA6::KanMX6 gtr1::KanMX6 gtr2::KanMX6 npr3:His3MX6 TetO7-GTR1-YCplac33-URA3 TetO7-gtr2-Q66L -YCplac111-LEU2)*	This paper	Figure 2
Strain 3798 (*MATa sch9: SCH9-HA6::KanMX6 lst4::His3MX6)*	This paper	Figure S3
Strain 4160 (*MATa sch9: SCH9-HA6::KanMX6 fba1::NatMX6 $TetO_{off}$-FBA1:URA3-YCplac33)*	This paper	Figure 3
Strain 4162*(MATa sch9: SCH9-HA6::KanMX6 fba1::NatMX6 $TetO_{off}$-FBA1:URA3-YCplac33 gtr1::KanMX6)*	This paper	Figure 3
Strain 4764 (*MATa sch9: SCH9-HA6::KanMX6 fba1::NatMX6 $TetO_{off}$-FBA1:URA3-YCplac33 npr3::His3MX6)*	This paper	Figure 3
Strain 4766 (*MATa sch9: SCH9-HA6::KanMX6 fba1::NatMX6 $TetO_{off}$-FBA1:URA3-YCplac33 npr3::His3MX6 gtr1::KanMX6)*	This paper	Figure 3
Strain 4503 (*MATa sch9: SCH9-HA6::KanMX6 tpi1::NatMX6)*	This paper	Figures 3 and S5
Strain 4505 (*MATa sch9: SCH9-HA6::KanMX6 tpi1::NatMX6 gtr1::KanMX6)*	This paper	Figures 3 and S5
Strain 4748 (*MATa sch9: SCH9-HA6::KanMX6 tpi1::NatMX6 npr3::His3MX6)*	This paper	Figure 3
Strain 4750 (*MATa sch9: SCH9-HA6::KanMX6 tpi1::NatMX6 npr3::His3MX6 gtr1::KanMX6)*	This paper	Figure 3
Strain 4574 (*MATa sch9: SCH9-HA6::KanMX6 pgk1::NatMX6)*	This paper	Figures 3 and 4
Strain 4576 (*MATa sch9: SCH9-HA6::KanMX6 pgk1::NatMX6 gtr1::KanMX6)*	This paper	Figure 3
Strain 4647 (*MATa sch9: SCH9-HA6::KanMX6 pgk1::NatMX6 npr3::His3MX6)*	This paper	Figure 3

(*Continued on next page*)

Continued

REAGENT or RESOURCE	SOURCE	IDENTIFIER
Strain 4630 (*MATa sch9: SCH9-HA6::KanMX6 pgk1::NatMX6 npr3::HIS3MX6 gtr1::KanMX6)*	This paper	Figure 3
Strain 4507 (*MATa sch9: SCH9-HA6::KanMX6 gpm1::NatMX6)*	This paper	Figure S6
Strain 4509 (*MATa sch9: SCH9-HA6::KanMX6 gpm1::NatMX6 gtr1::KanMX6)*	This paper	Figure S6
Strain 3951*(MATa sch9: SCH9-HA6::KanMX6 cdc19::NatMX6)*	This paper	Figure S6
Strain 3965 (*MATa sch9: SCH9-HA6::KanMX6 cdc19::NatMX6 gtr1::KanMX6)*	This paper	Figure S6
Strain 3818 (*MATa sch9: SCH9-HA6::KanMX6 pet100::NatMX6)*	This paper	Figure 4
Strain 3914 (*MATa sch9: SCH9-HA6::KanMX6 pet100::NatMX6 gtr1:KanMX6)*	This paper	Figures 4 and S7
Strain 4631 *(MATa sch9: SCH9-HA6::KanMX6 rho- petite 1 strain)*	This paper	Figure 4
Strain 4632 *(MATa sch9: SCH9-HA6::KanMX6 rho- petite 2 strain)*	This paper	Figure 4
Strain 4633 *(MATa sch9: SCH9-HA6::KanMX6 gtr1:KanMX6 rho- petite 1 strain)*	This paper	Figure 4
Strain 4634 *(MATa sch9: SCH9-HA6::KanMX6 gtr1:KanMX6 rho- petite 2 strain)*	This paper	Figure 4
Strain 4556 *(MATa sch9: SCH9-HA6::KanMX6 fba1::NatMX6 P_{ADH1}-H.s. AldA-pRS316-2μm)*	This paper	Figure 5
Strain 4558 (*MATa sch9: SCH9-HA6::KanMX6 fba1::NatMX6 P_{ADH1}-H.s. AldA-pRS316-2μm gtr1::KanMX6)*	This paper	Figure 5
Strain 4560 *(MATa sch9: SCH9-HA6::KanMX6 fba1::NatMX6 P_{ADH1}-H.s. AldA-pRS316-2μm npr3:HIS3MX6)*	This paper	Figure 5
Strain 4562 *(MATa sch9: SCH9-HA6::KanMX6 fba1::NatMX6 P_{ADH1}-H.s. AldA-pRS316-2μm npr3::HIS3MX6 gtr1::KanMX6)*	This paper	Figure 5
Strain 4189 (*MATa sch9: SCH9-HA6::KanMX6 cdc19::NatMX6 $TetO_{off}$-CDC19:URA3-YCplac33)*	This paper	Figure 5
Strain 4191 *(MATa sch9: SCH9-HA6::KanMX6 cdc19::NatMX6 $TetO_{off}$-CDC19:URA3-YCplac33 gtr1::KanMX6)*	This paper	Figure 5

(*Continued on next page*)

Continued

REAGENT or RESOURCE	SOURCE	IDENTIFIER
Strain 4223 *(MATa sch9: SCH9-HA6::KanMX6 cdc19::NatMX6 $TetO_{off}$-CDC19:URA3-YCplac33 npr3::HIS3MX6)*	This paper	Figure 5
Strain 5016 (*MATα sch9: SCH9-HA6::KanMX6 cdc19::NatMX6 $TetO_{off}$-cdc19-E392A R459Q:URA3-YCplac33)*	This paper	Figure 5
Strain 5017 *(MATα sch9: SCH9-HA6::KanMX6 cdc19::NatMX6 $TetO_{off}$- cdc19-E392A R459Q:URA3-YCplac33 gtr1::KanMX6)*	This paper	Figure 5
Strain 5106 *(MATa sch9: SCH9-HA6::KanMX6 cdc19::NatMX6 $TetO_{off}$- cdc19-E392A R459Q:URA3-YCplac33 npr3::His3MX6)*	This paper	Figure 5
Strain 3884 *(MATa sch9: SCH9-HA6::KanMX6 fbp1::NatMX6)*	This paper	Figure 5
Strain 4406 *(MATa sch9: SCH9-HA6::KanMX6 fbp1::NatMX6 gtr1::KanMX6)*	This paper	Figure 5
Strain 5102 (*MATa sch9: SCH9-HA6::KanMX6 fbp1::NatMX6 gtr1::KanMX6 npr3::His3MX6)*	This paper	Figure 5
Strain 4699 *(MATa sch9: SCH9-HA6::KanMX6 rav2::NatMX6)*	This paper	Figure 6
Strain 4701 *(MATa sch9: SCH9-HA6::KanMX6 rav2::NatMX6 gtr1::KanMX6)*	This paper	Figure 6
Strain 4842 (*MATa sch9: SCH9-HA6::KanMX6 vma5:: VMA5-GFP:NatMX6 vph1::VPH1-mCherry-NatMX6)*	This paper	Figure 6
Strain 5124 *(MATa sch9: SCH9-HA6::KanMX6 pgk1::NatMX6 vma5:: VMA5-GFP:NatMX6 vph1::VPH1-mCherry-NatMX6)*	This paper	Figure 6
Strain 5126 (*sch9: SCH9-HA6::KanMX6 tpi1::NatMX6 vma5:: VMA5-GFP:NatMX6 vph1::VPH1-mCherry-NatMX6)*	This paper	Figure 6
Strain 4402 *(MATa sch9: SCH9-HA6::KanMX6 ser3::NatMX6)*	This paper	Figure S7
Strain 4404 *(MATa sch9: SCH9-HA6::KanMX6 ser3::NatMX6 gtr1::KanMX6)*	This paper	Figure S7
Strain 4390 *(MATa sch9: SCH9-HA6::KanMX6 ser2::NatMX6)*	This paper	Figure S7
Strain 4392 *(MATa sch9: SCH9-HA6::KanMX6 ser2::NatMX6 gtr1::KanMX6)*	This paper	Figure S7
Strain 4408 (*MATa sch9: SCH9-HA6::KanMX6 gdh1::NatMX6 gdh2::HphMX6)*	This paper	Figure S7

(*Continued on next page*)

Continued

REAGENT or RESOURCE	SOURCE	IDENTIFIER
Strain 4410 (*MATa sch9: SCH9-HA6::KanMX6 gdh1::NatMX6 gdh2::HphMX6 gtr1::KanMX6)*	This paper	Figure S7
Strain 4835 *(MATa sch9: SCH9-HA6::KanMX6 npr3::His3MX6 pet100::NatMX6)*	This paper	Figure S7
Oligonucleotides		
Sequences of oligos used are listed in Table S1	This paper	N/A
Software and algorithms		
ImageJ	NIH	https://ImageJ.nih.gov/ij/
Prism	Graphpad software	https://www.graphpad.com/

RESOURCE AVAILABILITY

Lead contact

Further information and requests for resources and reagents should be directed to and will be fulfilled by the Lead Contact, Dr Prakash Arumugam (parumugam@sifbi.a-star.edu.sg).

Materials availability

Information and reagent requests will be fulfilled by the lead contact.

Data and code availability

- Data reported in this paper will be shared by the lead contact.
- This paper does not report original code.
- Any additional information required to reanalyze the data reported in this paper is available from the lead contact upon request.

EXPERIMENTAL MODEL AND STUDY PARTICIPANT DETAILS

Yeast strains and oligos

All yeast strains used in this study were generated from S. cerevisiae SK1 genetic background. A complete list of strains and genotype information is provided in the key resources table. The list of oligos used in study is provided in additional Table S1.

Chemical treatment to cell culture

Stock solution of rapamycin, antimycin A and bafilomycin A1 was prepared in dimethyl sulfoxide (DMSO). The final concentration of DMSO did not exceed 1% in experiments.

METHOD DETAILS

TORC1 activity assay

Overnight cells were grown in the medium at 30°C with 200 rpm shaking until they reached to logarithmic phase. Cells were then subjected to complete nutrient starvation by washing 3-times and incubating them in water at 30°C for 1 h. Starved cells were then transferred to appropriate experimental solutions. Aliquots of the cultures were collected at different time points and used for preparing protein extracts. Phosphorylation of Sch9 was monitored by western blotting as described previously.[16]

Quantification of western blot images

Quantification of Western blot band intensities was done with ImageJ (Fiji). Blot images were inverted to generate images for measurement of band intensities. A fixed Region Of Interest (ROI) per blot was set and integrated density values were measured for the top (phosphorylated) (ROI1) and bottom bands (ROI2). Final relative quantification values for phosphorylation per lane is expressed as a percentage of the values obtained for ROI1/(ROI1 + ROI2). Quantification data for Western blot images in Main and Supplementary Figures are presented in Tables S2 and S3 respectively.

Analysis of glycolytic metabolites

Glycolytic metabolites were extracted from logarithmic phase cells, starved cells and aliquots of cultures collected at different time points after the addition of carbon-source to starved cells. Cultures were quenched by mixing with twice the volume of methanol (pre-incubated at −80°C) and immediately spun down at 4500 rpm in centrifuge cooled to −10°C for 2 min. Supernatants were discarded and pellets were either stored at −20°C or processed further for metabolite extraction. Extraction solution, 40% (v/v) acetonitrile, 40% (v/v) methanol, and 20% (v/v) water was prepared and cooled to −80°C. All solvents used in extraction solution were HPLC grade. Extraction solution was mixed thoroughly prior to use. Pellets were resuspended with 700 μL cold extraction solution by pipetting up and down and kept on ice for 15 min. Mixture was spun down at highest speed in centrifuge cooled to -4°C for 5 min to remove cell debris. Supernatants were transferred to 1.5 mL microcentrifuge tube and evaporated to dryness in a vacuum evaporator or stored at −80°C. The dried extracts were redissolved in 100 μL of 98:2 water/methanol and analyzed by targeted liquid chromatography-mass spectrometry (LC-MS) analysis as previously described.[45]

ATP analysis

Yeast cells were mixed with the final concentration of 5% trichloroacetic acid (TCA) and then kept on ice for at least 5 min. Cells were washed and resuspended in 10% TCA and lysis was performed with glass beads in a bead beater to extract the ATP. The ATP level was quantified by PhosphoWorks Luminometric ATP Assay Kit (AAT Bioquest) and normalized by protein content measured by Bio-Rad protein assay kit.

Microscopy

Wild type, *tpi1Δ* and *pgk1Δ* cells expressing Vph1-mCherry and Vma5-GFP were grown to logarithmic phase at 30°C in YEP medium +2% Ethanol +2% Glycerol. Cultures were pelleted, washed, resuspended in water and starved for 1 h at 30°C. Glucose was added to a final concentration of 2% to starved cells. Aliquots of the cultures were taken after 15′ and 30′ and sonicated to disperse the cell clumps for easy microscopic visualization. 10 μL of cells was placed on a glass slide and directly visualized by differential interference contrast (DIC) and fluorescence microscopy using the Leica DM6000B microscope. Microscopic images were analyzed using the ImageJ software.

QUANTIFICATION AND STATISTICAL ANALYSIS

Data analysis of all the experimental results such as mean value, standard deviations, significance, and graphing was performed using GraphPad Prism v.9.3.1 software. The comparison of obtained results was statistically performed, and the graphs were plotted.